ACTIVE VIBRATION CONTROL OF SMART CURVED BEAM

A DISSERTATION

Submitted in partial fulfillment of the requirements for the award of the degree of

MASTER OF TECHNOLOGY

in

MECHANICAL ENGINEERING

(With Specialization in Machine Design Engineering)

By

UDAGIRI SANTOSH S.

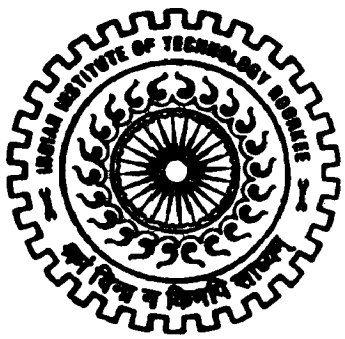

DEPARTMENT OF MECHANICAL AND INDUSTRIAL ENGINEERING
INDIAN INSTITUTE OF TECHNOLOGY ROORKEE
ROORKEE-247 667 (INDIA)

JUNE, 2006

CANDIDATE'S DECLARATION

I hereby declare that the work, which is being presented in this dissertation titled **"ACTIVE VIBRATION CONTROL OF SMART CURVED BEAM"** in the partial fulfillment of the requirements for the award of the degree of **Master of Technology** with the specialization in **Machine Design,** submitted in the Department of **Mechanical & Industrial Engineering, Indian Institute of Technology Roorkee, India,** is an authentic record of my own work carried out during the period from June 2005 to June 2006, under the supervision and guidance of **Dr. S.C. Jain,** Professor, Department of Mechanical & Industrial Engineering, IIT Roorkee, India.

I have not submitted the matter embodied in this dissertation for the award of any other degree.

Date: 29-06-06

Place: Roorkee

Udagiri S.

(Udagiri Santosh S.)

CERTIFICATE

This is to certify that the above statement made by the candidate is correct to the best of my knowledge and belief.

(Dr. S.C. Jain)
Professor,
Department of Mechanical &
Industrial Engineering
IIT Roorkee -247667, India.

ACKNOWLEDGEMENT

I am highly indebted to **Dr. S. C. Jain**, Professor, Department of Mechanical & Industrial Engineering, Indian Institute of Technology Roorkee, for encouraging me to undertake this dissertation as well as providing me all the necessary guidance and inspirational support throughout this dissertation work. He has displayed unique tolerance and understanding at every step of progress. It is my proud privilege to have carried out the dissertation work under his able guidance.

I am very grateful to **Prof V. K. Goel**, Head of the department of mechanical and industrial engineering, who supported my effort.

I express my gratitude to all the teachers of the department who had been source of inspiration to me and also to Mr. Rajeev Kumar, Research scholar, for his guidance.

I would like to thank my friends, for their help and encouragement at the hour of need. Finally I express my regards to my parents, brother who has been a constant source of inspiration to me.

29-06-06

(UDAGIRI SANTOSH S.)

ABSTARCT

In recent years, the strong demand for higher performance structures has driven a new development of smart materials and structures. Piezolaminated smart structures composed of passive elastic materials and active piezoelectric materials have been recently developed, which seem to be very promising in a variety of engineering application.

A finite element model of piezolaminated composite curved beam based on Timoshenko beam model and linear piezoelectric theory is presented. Finite element has three mechanical degree of freedom (u_0, w_0, θ_y) per node and one electrical degree of freedom per piezoelectric layer. Finite element has n-host structure layer and two piezoelectric layers. In deriving the finite element model of piezolaminated curved beam first displacement equation is given followed by strain displacement relationship, constitutive equation of piezoelectric, force and bending moment relation, strain energy equation, electrical energy equation, work done by external forces and electrical charges, kinetic energy equation. Governing equations are derived using Hamilton's principle Constant gain negative velocity feedback controller is used for vibration control. A neuro-controll also has been developed for controlling linear and non-linear structure. A code is developed in MATLAB for making numerical studies. Code is validated for static and dynamic analysis with the available literature.

Numerical studies is carried out in the reference of layered curved beam for the effect of radius of curvature on tip deflection, shape control, effect of actuator coverage area on tip deflection, active vibration control and application of neuro-controller on non-linear structure/plant.

Finally, it is observed that piezoelectric actuators can be used to control the shape of curved beam and a combination of sensor-actuator of controller can be used to control the vibration.

CONTENTS

NOMENCLATURE

A	Area of cross section
b	Width of beam in y direction
C	Structural damping
D	Electric displacement vector
$\overline{e}$	Piezoelectric stress coefficient
E	Electric field
f_s	Surface force intensity
F	Force
F_s	Overall Surface force
F_q	Overall force due to electrical charge
G	Shear modulus of material
G_c	Constant gain
h	Thickness of each layer in layered beam
I	Moment of inertia
k_s	Shear correction factor
K_{uu}	Stiffness matrix
$K_{u\Phi}$	Elastic electric coupling matrix
$K_{\Phi\Phi}$	Electric stiffness matrix
l	Length of beam
M	Bending moment
M_{uu}	Mass matrix
n	Number of layers
q	Surface electrical charge density
R	Radius of curvature of a Curved Beam
s	Dielectric tensor
S	Transverse shear force
S'_j	Total input to j^{th} hidden unit
q'_i	Total output to i^{th} hidden unit

T	Kinetic energy
t	Time
t_p	Thickness of piezoelectric layer
t_s	Thickness of piezoelectric sensor
t_a	Thickness of piezoelectric actuator
u	Displacement field in x direction
$\bar{u}$	Displacement vector at any point
u_0	Midplane displacement in x direction
V	Strain energy
V_p	Volume of piezoelectric layer
w	Displacement field in z direction
w_0	Midplane displacement in z direction
w'_{ij}	Weight between output layer (i) and hidden layer (j)
w'_{jk}	Weight between hidden layer (j) and input layer (k)
W	Work
W_e	Electrical energy
W_s	Work done by surface force
y_i	Output from i^{th} layer in neural network

Greek Symbols

ε	Strain field
ε_{xx}	Normal strain in x direction
ε_s	Shear strain
σ	Stress field
σ_{xx}	Stress in x direction
τ_{xz}	Transverse shear stresses
ξ	Natural co-ordinate
ν	Poisson ratio
Φ	Electric potential
ω	Frequency

ρ	Material density
θ	Threshold value
θ_y	Rotation about y axis
δ	Global Displacement vector
δ', α'	Newmark time integration parameters
η	Learning rate
α, β	Rayleigh's constant

Subscripts

a	Refers to the actuator
e	Refers to the element
s	Refers to the sensor
p	Refers to membrane or mid plane
b	Refers to bending
x	Relative to x direction
y	Relative to y direction
i, j, k	Refers to layers in neural network

Superscripts

T	Transpose of matrix

LIST OF FIGURES

LIST OF TABLES

CHAPTER 1

INTRODUCTION

1.1 Motivation:

Structural vibration suppression has attracted the attention of engineers since machines with moving parts and vehicles were invented. Especially the reductions of noise caused by structural vibrations and the diminishing of devastating vibrations have been of great interest. Passive and active control for structural vibration has been dramatically developed for both research and engineering applications in the past few decades. Effective vibration control is known to play an essential role in minimizing the risk of structural failure and improving the integral performance of systems.

Governed by the need of lightweight solutions for the aerospace industry, active vibration control techniques have experienced rapid developments in the last thirty years. While conventional approaches with passive damping materials minimize structural vibrations they add substantial amounts of weight to the structure and are minimized in their performance. However, active control techniques using smart materials offer light weight high performance solutions to vibration problems. Smart material based actuators and sensors are generally small and lightweight and hardly contribute to the total mass of the structure. Rising costs for gasoline and increased environmental concerns have compelled the automotive and aircraft industries to search for lighter damping solutions for their products. Decreasing the mass of passive damping materials in today's automobiles could lead to better fuel economy and, hence, lower the emission of greenhouse gases and pollution. Active vibration control systems retain low noise standards, while at the same time reducing the mass of passive damping materials. Containing more than one ton of passive vibration damping materials modern commercial airplanes are another example with a high potential for benefiting from reduced weight and decreased vibration and noise levels. Assuming a constant lift-off weight for an airplane, active vibration control can help to transport more cargo in one flight and, therefore, reduce the number of necessary flights. Both industries, the automotive and the aircraft are spending millions of Dollars every year on research for new lighter materials and new technologies like active vibration damping.

The field of smart structures has been an emerging area of research for the last few decades. Smart structures or intelligent structures can be defined as structures that are capable of sensing and actuating in a controlled manner in response to an input. The ability of the piezoelectric materials to convert electrical to mechanical energy and vice versa makes them to be employed as actuators and sensors. A variety of different materials can be utilized as either sensor or actuator elements in smart structure applications. Depending on the specific material used, the sensor and actuator elements are controlled through electric, magnetic, thermal, or light energy. Some of the common actuator and sensor materials include: piezoelectric materials, shape memory alloys, fiber optics, electrostrictive materials, magnetostrictive materials, and electro-rheological fluids. In piezoelectric materials electrical charge is produced due to mechanical strain, this is called the direct piezoelectric effect and mechanical strain is produced due to an applied electric field, which is called the converse piezoelectric effect. The coupled mechanical and electrical properties of piezoelectric materials make them well suited for use as sensors and actuators. Other advantages of piezoelectric materials which help account for their widespread popularity include: simple integration into the structure; a readily obtainable commercial supply of piezopolymers and piezoceramics. The two common types of piezoelectric materials are lead zirconate titanate (PZT) ceramics and polyvinylidene fluoride (PVDF) polymers. When used as actuators, these materials can be used to generate a secondary vibration response in a mechanical system, which could reduce the overall response, by destructive interference with the original response of the system, caused by the primary source of vibration.

This work deals with the modeling of a composite curved beam using finite element method assuming the Timoshenko beam theory. The dynamic characteristics of the structure are studied and piezoelectric layers are used to control its vibration. The vibration of the structure is controlled using constant gain negative velocity feedback controller. A neuro-controller is developed. Based on the training, this controller can be used for both linear and nonlinear control action.

1.2 Preamble

The primary objectives of this study are to develop a simple finite element for multilayered composite curved beam. The element has three mechancial degrees of freedom, two displacements and one slope, (i.e. shear rotations) per node and one electrical degree of freedom per piezoelectric layer. The accuracy of the element is demonstrated through the problems. In the present work the effect of radius of curvature on the tip deflection, shape control of composite curved beam, the effect of raidus of curvature on natural frequency, transient vibration control of composite curved beam and neuro-controller is developed for linear and non-linear control application.

1.3 Organization of the thesis:

Chapter 2 addresses background of smart material, piezoelectric constitutive relations and the strategies in the active vibration control have been discussed.

Chapter 3 contains a brief discussion regarding the previous work that has been done in this field. Summarized details of work carried out by different authors, their objectives and conclusions are given.

Chapter 4 details the development of the finite element model using the Timoshenko beam theory, the derivation of the equations is given in detail.

Chapter 5 discusses the basic terminology of Neural Network. The importance of neuro-controller in smart structure is explained. The back-propagation algorithm is discussed.

Chapter 6 presents the results and discussion part.

CHAPTER 2

BACKGROUND

This chapter covers the explanation regarding the smart structures which includes a brief description of the piezoelectricity and active control strategies for the vibration suppression.

2.1 Smart Materials

Materials of all kind play an important role in our society. It is obvious that new materials and applications are continuing to emerge. "Smart" materials are one of the emerging materials in today's development of material science and technology. The concept of smart materials indicates few more special functions which are not being found in traditional structural materials. Smart materials are thus defined that the material which one has capability to "feel" a stimulus and suitably react to it just like any living organism. Inanimate, as the material inherently is, it does not posses the capabilities of sensing and processing of stimulus and actuating the response [1].

Structural science and technology have made amazing developments in the design of electronics and machinery using standard materials, which do not have particularly special properties (i.e. steel, aluminum, gold). Imagine the range of possibilities, which exist for special materials that have properties scientists can manipulate. Some such materials have the ability to change shape or size simply by adding a little bit of heat, or to change from a liquid to a solid almost instantly when near a magnet; these materials are called "smart materials". In simple way we thus may define, the smart material that responds to change in temperature, moisture, electric and magnetic fields.

An Intelligent structure consists of four basic components

1. Structural system
2. Sensory system
3. Actuator system
4. Controls

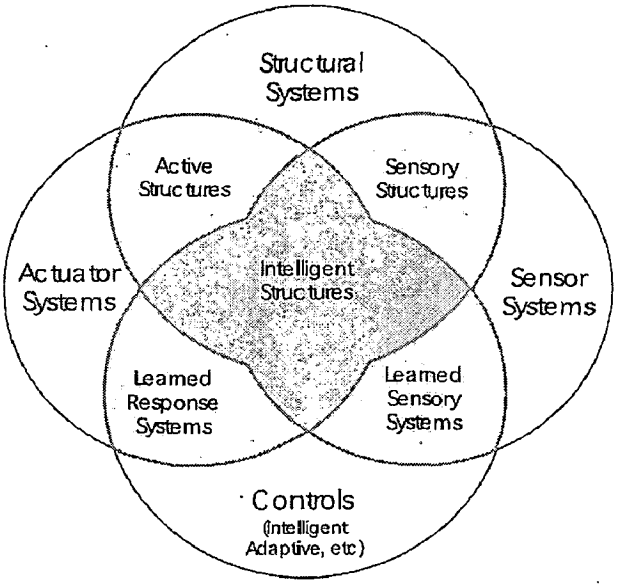

Fig 2.1 Intelligent Structure

Fig. 2.1 gives an illustration of an Intelligent Structure. Smart materials and structures are considered to possibly have the capability to contribute to vibration suppression of the structure, hence improved performance of the system. The following are strengthens of smart material/structures concluded from the research of the past.

Smart structures, with integrated sensors and actuator materials, might eliminate the need for heavy mechanical actuation systems or damping systems through their functionality for shape change or vibration control.

Smart structures are lighter in weight, consume less energy and achieve higher performance levels. They are important because they have the ability to take advantage of new advancing computer technologies and integrated sensor/actuators [2].

For vibration control purposes, a number of smart materials can be used as actuators and sensors such as piezoelectric materials, magneto-rheological materials, electro-rheological materials, and shape memory alloys (SMA).Here, we concentrate on using piezoelectric materials because they have good broadband sensing and actuation properties. Different smart materials include:

Piezoelectric Materials: Piezoelectricity is the ability of a material to develop an electrical charge when subjected to a mechanical strain and conversely. They have a

recoverable strain of 0.1% under electric field; they can be used as actuators as well as sensors. Examples are PZT, PVDF, etc.

Shape Memory Alloy (SMA): These materials appear attractive as actuators because of the possibility of achieving large excitation forces and displacements. These materials undergo phase transformation at a specific temperature. When plastically deformed at a low temperature, these alloys recover their original undeformed condition if the temperature is raised above the transformation temperature. This process can be repeated again. A remarkable characteristic of SMA is its large change of modulus of elasticity with heating (typically three to five times of the room temperature value). The most common SMA material is nitinol (nickel titanium alloy) and is available in the form of wires of different diameters. Though heating is carried out internally (electrically), response is very slow (less than 1Hz). Examples are Ni-Ti alloys, Cu-Zn-Al, Cu-Al-Ni, Fe-Mn, and Fe-Mn-Si, etc.

Electrostrictive Materials: These are quite identical to piezoelectric materials, with slightly better strain capability, but are very sensitive to temperature. Also, electrostrictive materials have a monopolar and nonlinear relation between electric field and induced strain. They exhibit negligible hysteresis. Piezoceramics can be elongated and compressed, while electrostrictive materials only exhibit an elongation, independent of the direction of the applied electric field.

Magnetostrictive Materials: As a magnetostrictive material is magnetized, there is a change in length. Conversely if an external force produces a strain in magnetostrictive materials, its magnetic state will change. Magnetostrictive materials have a recoverable strain of 0.15% under magnetic field; the maximum response is obtained when the material is subjected to compressive loads. These materials generate low strain and moderate forces over a wide frequency range. These materials are monopolar and nonlinear and exhibit hysteresis. Because of coil and magnetic return path, these actuators are often bulky. They can be used in high precision applications. Example is Terfenol-D.

Electro-Rheological (ER) Fluids and Magneto-Rheological (MR) Fluids: ER fluids are smart materials consisting of dielectric micro particles dispersed in an insulating liquid, usually silicon oil. When an external electric field is applied, they can be changed within a few milliseconds into a solid state but revert to liquids instantly when the current goes off. The phenomenon is so called ER effect. Magneto-Rheological (MR) fluids are comprised of micron sized iron particles that have been coated with anti coagulant material which are dispersed in an oil carrier. MR fluids experience a viscosity change when exposed to magnetic field. Examples of MR fluid is tiny iron particles suspended in oil and that of ER fluid are milk chocolate or cornstarch and oil [4].

Fiber Optics: This material is becoming popular as sensors because they can be easily embedded in composite structures with little effect on the structure integrity and also has potential of multiplexing. These fibers have relatively small diameters and can be embedded into the structure with negligible effects on the overall properties of the structure. In practical applications, a light source is sent into the network or grid of these fibers that are embedded in the structure. The signal is received at the other end and is processed or analyzed. Any changes in the light signal (phase, polarization, frequency, wavelength, intensity, etc.) would correspond to some mechanical changes in the structure. These sensors are useful in the health monitoring of the structure such as detecting cracks; and can also be designed to detect strains and other variables. A sophisticated network of fiber optics used in intelligent structures will be analogous to a nervous system of the structure. Another advantage of fiber optic is that it is virtually free from electromagnetic interference as well as having quite little energy loss from the transmission of light. Though it seems like an ideal sensor, its implementation might require embedding techniques which are non-trivial and the general engineering community has less than a high degree of familiarity with it [5].

2.1.2 Piezoelectric Materials

In 1880, Pierre and Paul-Jacques Curie discovered the direct piezoelectric effect on various crystals such as tourmaline, Rouchelle salt and quartz. The crystals generated electrical charges on their surfaces when they were mechanically strained in certain directions. In the following year, they also discovered the converse piezoelectric effect that the shape of crystals would change when an electric field was applied to them.

The ability of the piezoelectric materials to exchange electrical and mechanical energy opens up the possibility of employing them as actuators and sensors. If the piezoelectric materials are bonded properly to a structure, structural deformations can be induced by applying a voltage to the materials, employing them as actuators. On the other hand, they can be employed as sensors since deformations of a structure would cause the deformed piezoelectric materials to produce an electric charge. The extent of structural deformation can be observed by measuring the electrical voltage the materials produce. Unfortunately, the piezoelectric effect in natural crystals is rather weak so they cannot be used effectively as actuators or sensors.

However, recent developments in the field of materials science have provided piezoelectric materials that have sufficient coupling between electrical and mechanical domains. There are two broad classes of piezoelectric materials used in vibration control: ceramics and polymers. The piezopolymers are used mostly as sensors; because they require high voltages as well as they are lightweight and flexible so they are not effective as actuators on stiff structures. The best known is the polyvinylidene fluoride (PVDF). Piezoceramics are used extensively as actuators and sensors, for a wide range of frequency including ultrasonic applications. The best known piezoceramic is Lead Zirconate Titanate (PZT) [Pb (Zr, Ti) O_3]. PZT has larger electromechanical coupling coefficients than PVDF so PZT can induce larger forces or moments on structures. However, PZT is relatively brittle while PVDF is flexible and can be easily cut into any desired shape. PVDF also has good sensing properties so it is commonly used for sensors. Piezoelectric materials offer a number of advantages over conventional actuators like low energy consumption, fast response, high efficiency and compactness. But they have some limitations also like voltage that can be applied is limited in the range of-500 V to 1500V,

the piezo materials cannot be used above their curie temperature, which is 200°C to 300 °C due to possibility of depolarization.

2.1.3 Piezoelectricity

The piezoelectric effect is a property that exists in many materials. The name combines "piezo" which is derived from the Greek word for pressure, and "electric" from the Greek word for amber—static electricity generated by rubbing amber being the first known electric phenomenon. A rough translation is pressure-electric effect. In a piezoelectric material, the application of a force or stress results in the development of a charge in the material. Conversely, the application of a charge to the same material will result in a change in mechanical dimensions or strain.

Several ceramic materials exhibit a piezoelectric effect. These include lead-zirconate-titanate (PZT), lead-titanate ($PbTiO_2$), lead-zirconate ($PbZrO_3$), and barium-titanate ($BaTiO_3$). Strictly speaking, these ceramics are not actually piezoelectric but rather exhibit a polarized electrostrictive effect.

A material must be formed as a single crystal to be truly piezoelectric. Ceramics have a multi-crystalline structure made up of large numbers of randomly orientated crystal grains. The random orientation of the grains results in a net cancellation of the piezoelectric effect. The ceramic must be polarized to align a majority of the individual grain's effects. Nonetheless, the term "piezoelectric" has become interchangeable with "polarized electrostrictive effect" in most literature.

Poling

Piezoelectric ceramic materials are not piezoelectric until the random ferroelectric domains are aligned. This alignment is accomplished through a process known as poling. Poling consists of inducing a DC voltage across the material. The ferroelectric domains align to the induced field resulting in a net piezoelectric effect. It should be noted that not all the domains become exactly aligned. Some of the domains only partially align and some do not align at all. The number of domains that align depends upon the poling voltage, temperature, and the time the voltage is held on the material.

During poling the material permanently increases in dimension between the poling electrodes and decreases in dimensions parallel to the electrodes. The material can be de-poled by reversing the poling voltage, increasing the temperature beyond the material's Currie point, or by inducing a large mechanical stress.

Post Poling

Applied voltage:

Voltage applied to the electrodes at the same polarity as the original poling voltage results in a further increase in dimension between the electrodes and decreases the dimensions parallel to the electrodes. Applying a voltage to the electrodes in an opposite direction decreases the dimension between the electrodes and increases the dimensions parallel to the electrodes.

Applied force:

Applying a compressive force in the direction of poling (perpendicular to the poling electrodes) or a tensile force parallel to the poling direction results in a voltage generated on the electrodes that has the same polarity as the original poling voltage. A tensile force applied perpendicular to the electrodes or a compressive force applied parallel to the electrodes results in a voltage of opposite polarity.

Shear:

Removing the poling electrodes and applying a field perpendicular to the poling direction on a new set of electrodes will result in mechanical shear. Physically shearing the ceramic will produce a voltage on the new electrodes.

2.1.4 Piezoelectric constitutive relations

Piezoceramic materials are assumed to be linear and the actuation strain is modeled like thermal strain. Piezoceramics can be idealized as an orthotropic material such as unidirectional laminated composite. The constitutive relations are based on the assumption that the total strain in the actuator is the sum of the mechanical strain induced by the stress, the thermal strain due to temperature and the controllable actuation strain due to electric voltage.

The axes are identified by numerals: 1 corresponding to x-axis, 2 corresponding to y-axis and 3 corresponding to z-axis .A piezoelectric material produces strains when an electric field is applied along its poling direction, which is generally along the 3-direction for a monolithic-type material Conversely, it generates electric displacement when it is strained. While the former property is used in actuation, the latter is used in sensing. Fig. 2.2 shows the axis configuration of piezoelectric patch describing the directions of applied electric field.

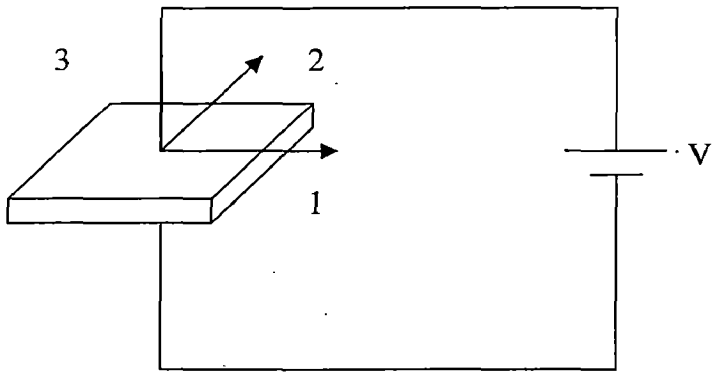

Figure 2.2 Axis Configuration of Piezoelectric Patch

Coupled electromechanical constitutive relations are:

$$\{\sigma\}=[Q]\{\varepsilon\}-[e]^T\{E\} \tag{2.1}$$

$$\{D\}=[e]\{\varepsilon\}+[s]\{E\} \tag{2.2}$$

Where

$\{\sigma\}$ = Stress vector

$\{\varepsilon\}$ = Strain vector

$[Q]$ = Elasticity constant matrix

$\{E\}$ = Electric field

$\{D\}$ = Electric displacement

$[e]$ = Piezoelectric constant stress matrix

$[s]$ = Dielectric constant matrix

Rewriting above equation

$$\begin{Bmatrix} D_1 \\ D_2 \\ D_3 \end{Bmatrix} = \begin{bmatrix} 0 & 0 & 0 & 0 & d_{15} & 0 \\ 0 & 0 & 0 & d_{24} & 0 & 0 \\ d_{31} & d_{32} & d_{33} & 0 & 0 & 0 \end{bmatrix} \begin{Bmatrix} \varepsilon_1 \\ \varepsilon_2 \\ \varepsilon_3 \\ \varepsilon_{23} \\ \varepsilon_{13} \\ \varepsilon_{12} \end{Bmatrix} + \begin{bmatrix} s_{11} & 0 & 0 \\ 0 & s_{22} & 0 \\ 0 & 0 & s_{33} \end{bmatrix} \begin{Bmatrix} E_1 \\ E_2 \\ E_3 \end{Bmatrix} \quad (2.3)$$

Where d_{33}, d_{31} and d_{15} are called piezoelectric strain coefficient of a mechanical free piezo element.

- d_{31} Characterizes strain in the 1 and 2 directions due to an electric field E_3 in the 3 direction
- d_{33} Characterizes strain in the 3 direction due to field in the 3 direction.
- d_{15} Relates shear strains in 2-3 and 3-1 planes due to field respectively.

Thus, if an electric field E_3 is applied to a free piezo-element, it causes longitudinal strains ε_1, ε_2 and ε_3. If an electric field E_1 or E_2 is applied, the material reacts with shear strain γ_{31} and γ_{23} respectively.

If a compressive force is applied in the polarization direction (axis 3), or tensile force is applied in the plane perpendicular to polarization direction (axis 2 or 1), it will result in a voltage that has the same polarity as the original poling direction.

During the manufacture of a piezoceramic, a large (greater than 1 kV/mm) field is applied across the ceramic to create polarization. This is called coercive field during subsequent testing, if the field greater than coercive field, is applied opposite to the polarization direction, the ceramic will lose its piezoelectric properties. This phenomenon is called depoling. However, it is possible to repole the material. If an applied electric field is aligned with the initial polarization direction, there is no depoling sufficient high voltage can cause arcing or a brittle fracture. Poling is also possible if high temperature or large stress is applied.

2.2 Active control strategies for vibration suppression

Active vibration control using smart structures is used to reduce the vibrations of a system by automatic modifications of the systems structural response. Smart structures are man-made engineered systems that mimic nature's ability to react to stimuli. Active vibration control is widely used because of its broad frequency response range, low additional mass, high adaptability and good efficiency. Figure 2.3shows a typical active control system. It consists of sensors, which are used to monitor the mechanical response of the structure through changes in the displacements, strains, or accelerations. Once an adverse or undesirable structural response is detected in the sensors, a controller generates the required input to the actuators. The actuators respond to this input and produce a corresponding change in the mechanical response of the structure to a more acceptable state.

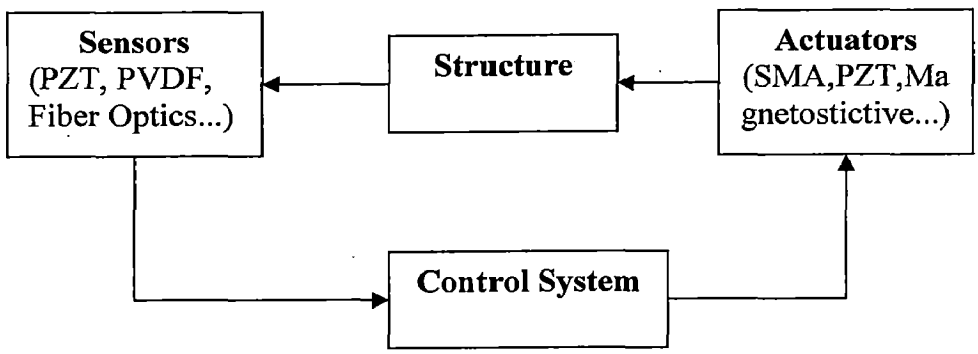

Figure 2.3 An Active Control System [2]

The capability of smart structures to sense and adapt to their environment leads to a wide range of potential applications including: vibration suppression of aircraft structures; noise control of helicopter rotors; health monitoring of bridges; shape control of large space trusses [2].

CHAPTER 3

LITERATURE REVIEW

In recent years many modeling and control techniques for smart structures have been proposed. This chapter offers a review of the current literature. The purpose of this chapter is to present a short survey of smart curved beam modeling using surface mounted sensors / actuators. In the latter part the application of Neural Network in the area of smart structure is surveyed.

Ryu D. H., and Wang K.W. [20] has evaluated the effectiveness of different types and configurations of surface-bonded piezoelectric actuators on curved beams. Firstly, an analytical model for curved piezoelectric actuators is developed to investigate the actuation mechanism, considering the effects of the interfacial stresses as well as shear stresses. The average value of the moment distribution calculated from the interfacial stresses is used as a performance index to evaluate the actuation authority, treating the piezoelectric patch as a point moment actuator. Secondly, for the analysis of flat actuators, a three–dimensional finite element method is used to include the effects of interfacial peeling stresses. Finally, experiments are carried out to verify the numerical model. The results shows that effects of interfacial peeling stresses should be considered under certain conditions depending on the system parameters, especially when the thickness of the host structure is relatively thin.

M.H.H. Shen [32] has been proposed a one-dimensional mathematical model for determining the mechanical responses of beams with piezoelectric actuators. This model is based on Timoshenko beam theory with the host beam and piezoelectric patches being separately modelled using beam elements.

Hui-Ru Shih [19] has presented the distributed vibration sensing and control of piezoelectric laminated curved beam. The mathematical model of curved beam with a distributed piezoelectric sensor and actuator is formulated first, followed by vibration analysis. This model provides estimates of the sensor signal, actuator-induced membrane force, and actuator-induced bending moment, as well as predicting the controlled

damping ratio and dynamic response. The sensor sensitivity with various sensor thicknesses is studied and compared.

P. Seshu, V.K.Gupta [23] has been developed a shell finite element formulation to model typical smart antenna shell structures incorporating piezoelectric actuators for their shape control. This element has been used to study the behavior of support curved beams under piezoelectric actuation. Experiments have been conducted to study static actuation of straight and curved beams under varying amplitude of field.

Balamurugan, V. and Narayanan, S. [22] have dealt with the active vibration control offceam like structure with distributed piezoelectric sensor and actuator layers bonded on top and bottom surfaces of the beam. A finite element model based on Bernoulli-Euler beam theory has been developed. The contribution of the piezoelectric sensor and actuator layer on the mass and stiffness of the beam is considered. Three types of classical control strategies, namely direct proportional feedback, constant-gain negative feedback and Liyapunov feedback and an optimal strategy, Linear Quadratic Regulator (LQR) scheme are applied to study their control effectiveness.

Balamurugan, V. and Narayanan, S. [9] has dealt with finite element modelling of laminated structures with distributed piezoelectric sensor and actuator layers and control electronics. The effects of temperature on the electrical and mechanical properties and the coupling between them are also taken in to consideration in the finite element formulation. The formulations are based on the first order deformation theories. Constant-gain negative feedback and Liyapunov feedback and an optimal strategy, Linear Quadratic Regulator (LQR) approach are used for active vibration control with structures subjected to impact, harmonic and random excitations. The influence of pyroelectric effects on the vibration control is investigated. The LQR approach is found to be more effective in vibration control with lesser peak voltages applied in the piezo actuator layers as in this case control gains are obtained by minimizing a performance index

Sudhakar A. Kulkarni, Kamal M. Bajoria [8], have presented a finite element formulation of a degenerate shell element, using higher order shear deformation theory.

An eight-noded element is used to derive global coupled electro elastic behavior of the overall structure. The model incorporates the warping of cross section due to transverse shear stresses and assumes a parabolic shear strain variation over the thickness. The static deflections of bimorph beam are compared with the literature. Active vibration control performance of the piezolaminated curved beam with distributed sensors and actuators is studied. The variation of the damping effect with different gains and actuator coverage is studied.

Snyder and Tanaka [24] developed a nonlinear feedforward controller for smart structures, and they showed that the neural network is essentially a transversal filter with a nonlinear hidden layer between the input and output.

Chen ef al. [25] presented a numerical study related to the active control of the vibrations of a cantilevered beam with piezoelectric actuators using Modified Modal Space Control (M.I.M.S.C.) algorithm coupled with Neural Network for state estimation. The neural network state estimation for this modal parameter has to be designed with training data given by numerical simulation of the M.I.M.S.C. algorithm. The design takes place through the implementation of back propagation algorithm.

Vital Rao and Damle et al. [26] presented some of the structural identification and robust control methods used for smart structure applications. Experimental results of both identification and robust control of two smart structure test articles has been presented. A new adaptive learning rate algorithm and an adaptive neuron have been introduced to enhance learning in multi-layered neural networks.

Yi-Kwei Wen, Jamshid Ghaboussi, Paolo Venini and Khashayar Nikzad [27] have presented a method of control of structures based on neural networks. Analytical and experimental investigations have been discussed and finally numerical examples are given of control of a non-linear single degree of freedom structure by neural net.

James Douglas Schieffer and Kelvin Erickson [28] have developed a neur-ocontroller to control the vibration of a cantilever beam. The neural network uses only past tip position to predict the position of cantilever beam tip for the next five samples.

The output of the neural net structure is then used to calculate predictions of the velocity and acceleration are then used to calculate the voltage needed to excite piezo-ceramic actuators in order to bring the beam back to its steady state. The controller brings the beam back to resting position when subjected to impulse and a random input to the beam significantly faster than when the beam has no control.

K.Chandrashekhara, M.T.Valoor and S.Agarwal [29] have developed a self adapting vibration control system is developed. A hybrid system comprised of a dynamical diagonal recurrent neural network and an adaptive feedforward neural network is used to control the beam vibrations. A finite element model based on shear deformation theory is used to simulate the vibration response of laminated composite beams with integrated piezoelectric sensors and actuators. A robustness study including the effects of tip mass, structural parameter variation and partial loss of sensor output is performed.

Ratneshwar jha and Chengli He [30] has presented a comparison of neuro-controller with standard LQR control system for vibration reduction. Controller performances are tested using an experimental setup employing a cantilevered plate with surface bonded PZT actuators. The result shows that the neural adaptive predictive controller is very promising in terms of control effectiveness and control effort in the vibration suppression of smart structures.

Gwo-Shing Lee [14] has implemented neural networks to system identification and vibration suppression of smart structures. Three neural networks are developed, one for system identification, the second for online state estimation, and the third for vibration suppression. It is shown both in analysis and in experiment that these neural networks can identify, estimate, and suppress the vibration of a composite structure with embedded piezoelectric sensor and actuator.

CHAPTER 4

FEM FORMULATION

There are two FEM models available for Beams. In Euler Bernoulli Beam Theory the assumption made is, plane cross section before bending remains plane and normal to the neutral axis after bending. Timoshenko Beam Theory corrects the simplifying assumptions made in Euler Bernoulli Beam theory. In this theory cross sections remain normal to the deformed longitudinal axis. The deviation from normality is produced by a transverse shear is assumed to be constant over cross section [6]. Thus the Timoshenko Model is superior than Euler Bernoulli model in precisely predicting the beam response. Timoshenko beam theory is used in this work to generate the FE model of cantilever curved layered beam with distributed on both side by piezoelectric material

Piezoelectric elements can be incorporated into a laminated composite structure, either by embedding them or by mounting them onto the surface of the host structure. Surface mounted piezoceramic elements are usually bonded to the surface of a structural element and transfer stresses to the structural member according to the magnitude of the excitation voltage applied to them. There are two beam models in common use in structural mechanics, these are as follows

4.1 Euler-Bernoulli (EB) Model

This is called classical beam theory or engineering beam theory. This model accounts for bending moment effects on stresses and deformations. The effect of transverse shear forces on beam deformation is neglected. Its fundamental assumption is that cross sections remain plane and normal to the deformed longitudinal axis as shown in fig.4.1. The rotation θ is due to bending stress alone neglecting the transverse shear stress. This rotation occurs about a neutral axis that passes through the centroid of the cross section [3].

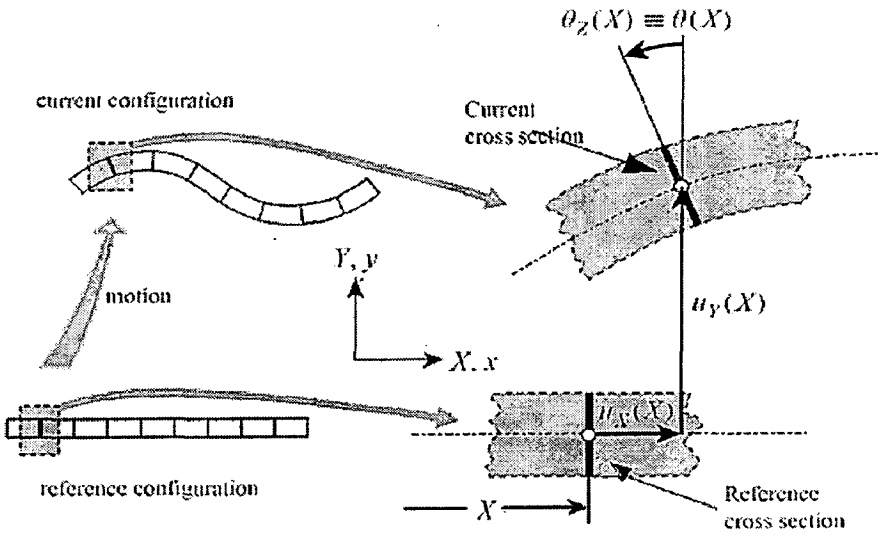

Figure 4.1 Euler Bernoulli Beam Model [3]

4.2 Timoshenko Beam Model

In this theory cross sections remain plane and rotate about the same neutral axis as the EB model, but do not remain normal to the deformed longitudinal axis as shown in fig.4.2. The deviation from normality is produce by a transverse shear that is slope of the beam consists of two parts, one due to bending and other due to shear [3].

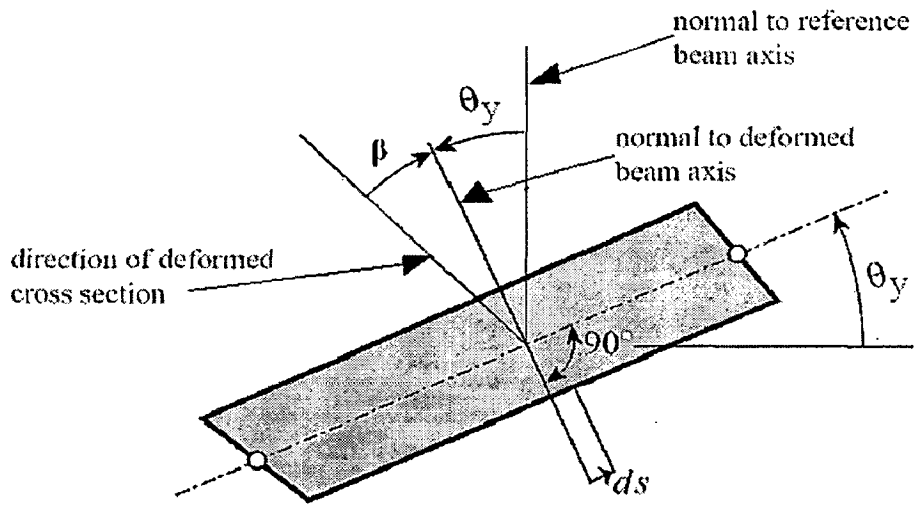

Figure 4.2 Timoshenko Beam Model [3]

4.3 Displacement Function

Using the assumptions of Timoshenko beam model [6], displacement field is given as:

$$u(x,z,t) = u_0(x,t) + z\theta_y(x,t) \qquad w(x,z,t) = w_0(x,t) \tag{4.1}$$

where (u_0, w_0) are the displacements of a point on the mid-plane of beam, and θ_y is the rotation (about the y-axis) of a transverse normal line as shown in fig 4.3.

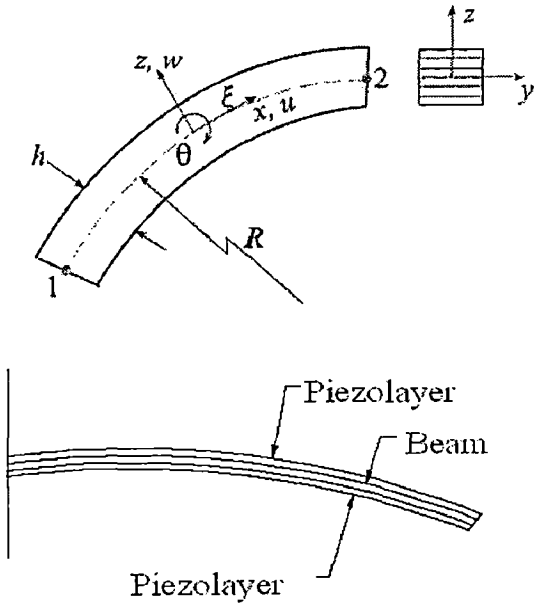

Figure.4.3 Geometry and co-ordinate systems of beam element

One-dimensional interpolation (shape) functions are used to define the geometry field at any point in the element. These shape functions relate the curvilinear coordinates in the nodal Cartesian coordinate system to the element coordinate system. These shape functions are,

$$N_1(\xi) = \frac{1}{2}(1-\xi) \qquad N_2(\xi) = \frac{1}{2}(1+\xi) \tag{4.2}$$

The element has three elastic degrees of freedom u_0, w_0 and θ_y per node.

$$\{\delta_i\}_e = \{u_{0i} \quad w_{0i} \quad \theta_{yi}\}^T \qquad i = 1, 2 \tag{4.3}$$

where u_{0i}, w_{0i} are the displacements along x and z axes respectively at node i and θ_{yi} is the rotation of normal about y-axis of node **i**.

Using the shape functions, one can define all field variables as follows,

$$u=\sum_{i=1}^{2}N_i u_{0i}+N_i z\theta_{yi} \qquad w=\sum_{i=1}^{2}N_i w_{0i} \qquad \theta_y=\sum_{i=1}^{2}N_i\theta_{yi} \tag{4.4}$$

Field variables can be written in matrix form as follows,

$$\{\bar{u}\}=\begin{Bmatrix}u\\ w\\ \theta_y\end{Bmatrix}=\begin{bmatrix}N_1 & 0 & zN_1 & N_2 & 0 & zN_2\\ 0 & N_1 & 0 & 0 & N_2 & 0\\ 0 & 0 & N_1 & 0 & 0 & N_2\end{bmatrix}\begin{Bmatrix}u_{01}\\ w_{01}\\ \theta_{y1}\\ u_{02}\\ w_{02}\\ \theta_{y2}\end{Bmatrix}=[N_u]\{\delta\}_e \tag{4.5}$$

4.4 Strain-displacement relationship

The strain displacement relationship is given as,

$$\varepsilon_{xx}=\frac{\partial u}{\partial x}=\left(\frac{\partial u_{0i}}{\partial x}+\frac{w}{R}\right)+z\frac{\partial\theta_{yi}}{\partial x},\ \varepsilon_{xx}=\varepsilon_p+z\varepsilon_b \tag{4.6}$$

Where,

$$\varepsilon_p=\left(\frac{\partial u_{0i}}{\partial x}+\frac{w}{R}\right),\ \varepsilon_b=\frac{\partial\theta_{yi}}{\partial x},\ \varepsilon_s=\frac{\partial w}{\partial x}+\frac{\partial u}{\partial z}-\frac{u_0}{R} \tag{4.7}$$

Above equation can be written as,

$$\varepsilon_p=\begin{bmatrix}\frac{\partial N_1}{\partial x} & N_1 & 0 & \frac{\partial N_2}{\partial x} & N_2 & 0\end{bmatrix}[u_{01}\ \ w_{01}\ \ \theta_{y1}\ \ u_{02}\ \ w_{02}\ \ \theta_{y2}]^T=[B_a]\{\delta\}_e \tag{4.8}$$

$$\varepsilon_b=\begin{bmatrix}0 & 0 & \frac{\partial N_1}{\partial x} & 0 & 0 & \frac{\partial N_2}{\partial x}\end{bmatrix}[u_{01}\ \ w_{01}\ \ \theta_{y1}\ \ u_{02}\ \ w_{02}\ \ \theta_{y2}]^T=[B_b]\{\delta\}_e \tag{4.9}$$

$$\varepsilon_s=\begin{bmatrix}-\frac{N_1}{R} & \frac{\partial N_1}{\partial x} & N_1 & \frac{N_2}{R} & \frac{\partial N_2}{\partial x} & N_2\end{bmatrix}[u_{01}\ \ w_{01}\ \ \theta_{y1}\ \ u_{02}\ \ w_{02}\ \ \theta_{y2}]^T=[B_s]\{\delta\}_e \tag{4.10}$$

where $[B_a]$, $[B_b]$ and $[B_s]$ are the matrix in terms of shape function and its derivative.

4.5 Constitutive equations of piezoelectric materials

The linear equations coupling elastic field and electric field in piezoelectric medium are expressed by the direct and converse piezoelectric equations, respectively.

$$\{\sigma\}=[Q]\{\varepsilon\}-[e]^T\{E\} \tag{4.11}$$

$$\{D\}=[e]\{\varepsilon\}+[s]\{E\} \tag{4.12}$$

where $[Q]$ = transformed stiffness matrix = $[T]^T[\bar{Q}][T]$

$$[T]=\begin{bmatrix}\cos^2\theta & 0\\ 0 & \cos\theta\end{bmatrix}$$

$[e]$ = transformed piezoelectric constant matrix= $[T]^T[\bar{e}]$

$[\bar{e}]$ = piezoelectric constant value

$$[\bar{Q}]=\text{stiffness matrix}=\begin{bmatrix}\dfrac{E_1}{(1-\nu_{12})(1-\nu_{21})} & 0\\ 0 & G_{13}\end{bmatrix}$$

The present element has three degrees of freedom $u_{0i}, w_{0i}, \theta_{yi}$ per node and one electrical degree of freedom, ϕ per element per piezoelectric layer. The electric field can be written as,

$$\{E\}=\begin{Bmatrix}E_x\\ E_y\\ E_z\end{Bmatrix}=-\begin{Bmatrix}\dfrac{\partial\phi}{\partial x}\\ \dfrac{\partial\phi}{\partial y}\\ \dfrac{\partial\phi}{\partial z}\end{Bmatrix}=-\begin{bmatrix}0 & 0\\ 1/t_s & 0\\ 0 & 0\\ 0 & 1/t_a\end{bmatrix}\begin{Bmatrix}\phi_s\\ \phi_a\end{Bmatrix}=-[B_\phi]\{\phi\} \tag{4.13}$$

Where t_s and t_a are thickness of piezoelectric sensor and actuator respectively.

4.6 Force and Bending Moment

For a piezolaminated composite laminate, if $\{F\}$ represents the membranes stress resultants and $\{M\}$ represents the bending stress resultants for n layers will be written as,

$$\{F\} = \int_{-h/2}^{+h/2} \sigma dz = \sum_{k=1}^{n} \int_{h_{k-1}}^{h_k} \sigma_{xx}\, dz \qquad \{M\} = \int_{-h/2}^{+h/2} \sigma\, z\, dz = \sum_{k=1}^{n} \int_{h_{k-1}}^{h_k} \sigma_{xx}\, z \quad dz \tag{4.14}$$

From equations (4.11), (4.12), (4.13) equation (4.14) reduces to,

$$\begin{aligned} \{F\} &= [A]\{\varepsilon_p\} + [B]\{\varepsilon_b\} - \int_{t_p} [e]^T \{E\}\, dz \\ \{M\} &= [B]\{\varepsilon_p\} + [D]\{\varepsilon_b\} - \int_{t_p} z\, [e]^T \{E\}\, dz \end{aligned} \tag{4.15}$$

where

$$[A] = \sum_{k=1}^{n} \int_{h_{k-1}}^{h_k} [Q]_k\, dz \quad [B] = \sum_{k=1}^{n} \int_{h_{k-1}}^{h_k} [Q]_k\, z\, dz \quad [D] = \sum_{k=1}^{n} \int_{h_{k-1}}^{h_k} [Q]_k\, z^2\, dz \tag{4.16}$$

The transverse shear stresses of the k_{th} lamina can be written as,

$$\{\tau_{xz}\} = [Q]\{\varepsilon_s\}_k \tag{4.17}$$

If $\{S\}$ represents transverse shear force resultant then,

$$\{S\} = \int_{-h/2}^{+h/2} \{\tau_{xz}\}\, dz = [E_s]\{\varepsilon_s\} \tag{4.18}$$

Where $[E_s]$ is shear stiffness coefficients of laminate given by,

$$[E_s] = \sum_{k=1}^{n} k_S{}^2 \int_{h_{k-1}}^{h_k} [Q]_k dz \tag{4.19}$$

Where k_s is shear correction factor [7].

4.7 Energy Formulation

4.7.1 Strain Energy

Using the Variational principle the strain energy functional, V is given by

$$V = \frac{1}{2}\int_A (\{\varepsilon_p\}^T\{F\} + \{\varepsilon_b\}^T\{M\} + \{\varepsilon_s\}^T\{S\})\, dA - \int_{V_p} (\{\varepsilon_p\}^T + z\{\varepsilon_b\}^T)[e]^T\{E\}^T\, dV \tag{4.20}$$

$$V = \frac{1}{2}\{\delta\}_e^T\,[K_{uu}]\{\delta\}_e + \frac{1}{2}\{\delta\}_e^T[K_{u\phi}]_e\{\phi\}_e \tag{4.21}$$

$$[K_{uu}]_e = \int_0^l b\,[[B_a]^T[A][B_a] + [B_b]^T[B][B_b] + [B_b]^T[B][B_a] + [B_b]^T[D][B_b] + [B_s]^T[E_s][B_s]]\, dl$$

$$[K_{u\phi}]_e = \int_{V_p} [[B_a]^T[e]^T[B_\phi]^T + z[B_b]^T[e]^T[B_\phi]]\, dV \tag{4.22}$$

where $[K_{uu}]_e$ the element stiffness matrix is$[K_{u\phi}]_e$ is the element elastic-electric coupling stiffness matrix and b is width of beam.

4.7.2 Electrical Energy Equation

Using constitutive relations, strain displacement and electric field electric-potential relations, the element electrical energy can be written as,

$$W_e = \frac{1}{2}\int_{V_p} \{E\}^T\{D\}dV \tag{4.23}$$

where, V_p is volume of piezoelectric layer.

$$W_e = -\frac{1}{2}\int_{V_p} \{\phi\}_e^T[B_\phi]^T[e][[B_a] + z[B_b]]\{\delta\}\, dV - \frac{1}{2}\int_{V_p} \{\phi\}_e^T[B_\phi]^T[s][B_\phi]\{\phi\}_e\, dV \tag{4.24}$$

$$W_e = -\frac{1}{2}\{\phi\}_e^T[K_{\phi u}]\{\delta\}_e - \frac{1}{2}\{\phi\}_e^T[K_{\phi\phi}]\{\phi\}_e \tag{4.25}$$

where $([K_{\phi u}]=[K_{u\phi}]^T)$ is element elastic-electric coupling stiffness matrix and $[K_{\phi\phi}]$ is element electric stiffness matrix.

4.7.3 Work done by external forces and electric charge

The work done by the surface force and the applied electrical charge density is given by

$$W_s = \int_A \{\overline{u}\}^T \{f_s\}\, dA - \int_A [E]^T \{q\}\, dA \tag{4.26}$$

Where $\{f_s\}$ and $\{q\}$ are the surface force intensity and surface electrical charge density, respectively. The above equation can be written as

$$W_s = \{\delta\}_e^T \{F_s\}_e + \{\phi\}_e^T \{F_q\}_e \tag{4.27}$$

Where, $\{F_s\}_e$ is an applied mechanical force in an element due to surface forces and are the $\{F_q\}_e$ applied electrical charge in an element.

4.7.4 Kinetic energy equation

The element kinetic energy is

$$T = \frac{1}{2} m\dot{u}_0^2 + \frac{1}{2} m\dot{w}^2 + \frac{1}{2} I\dot{\theta}_y^2 \tag{4.28}$$

Where,

$$\{\dot{u}_0\} = [N_u]\{\dot{\delta}\}_e \quad \{\dot{w}\} = [N_w]\{\dot{\delta}\}_e \quad \{\dot{\theta}_y\} = [N_{\theta_y}]\{\dot{\delta}\}_e \tag{4.29}$$

$$T = \frac{1}{2}\{\dot{\delta}\}_e^T b \int_0^l [P([N_u]^T[N_u] + [N_w]^T[N_w]) + I([N_{\theta_y}]^T[N_{\theta_y}])]\, dl \{\dot{\delta}\}_e \tag{4.30}$$

Where,

$P = \sum_{k=1}^{n} \int_{-h_{k-1}}^{h_k} \rho dz$, $I = \sum_{k=1}^{n} \int_{-h_{k-1}}^{h_k} z^2 \rho dz$ and n is the number of layers

$$T = \frac{1}{2}\{\dot{\delta}\}_e^T [M_{uu}]\{\dot{\delta}\}_e \tag{4.31}$$

where $[M_{uu}]$ is element mass matrix.

4.8 Equation of motion

Hamilton's principle assumes that the energy variation over an arbitrary period of time is zero. Using Hamilton principle, the governing equation for an element can be written as

$$\int_t \partial(T - V + W)dt = 0 \tag{4.32}$$

Putting equations (4.21), (4.25), (4.27) and (4.31) in equation (4.32), we get following global equations of motion and is given by,

$$[M_{uu}]_e\{\ddot{\delta}\}_e + [K_{uu}]_e\{\delta\}_e + [K_{u\phi}]_e\{\phi\}_e = \{F_s\}_e \tag{4.33}$$

$$[K_{\phi u}]_e\{\delta\}_e + [K_{\phi\phi}]_e\{\phi\}_e = \{F_q\}_e \tag{4.34}$$

The eq. (4.34) can be written as,

$$\{\phi\}_e = [K_{\phi\phi}]_e^{-1}\{F_q\}_e - [K_{\phi\phi}]_e^{-1}[K_{\phi u}]_e\{\delta\} \tag{4.35}$$

Substituting eq. (4.35) in eq. (4.34) we get,

$$[M_{uu}]_e\{\ddot{\delta}\}_e + [[K_{uu}]_e - [K_{u\phi}]_e[K_{\phi\phi}]_e^{-1}[K_{\phi u}]_e]\{\delta\}_e = \{F_s\}_e - [K_{u\phi}]_e[K_{\phi\phi}]_e^{-1}\{F_q\}_e \tag{4.36}$$

When eq. (4.34) is applied to sensors where the external applied charge is zero, the sensed voltage is given by

$$\{\phi_s\}_e = -[K_{\phi\phi}]_{se}^{-1}[K_{\phi u}]_{se}\{\delta\}_e \tag{4.37}$$

Subscript 's' denotes the sensor layer. In general, all the structures are lightly damped. Hence adding the artificial linear viscous damping the global equations of motion can be obtained by assembling the elemental equations and is given by,

$$[M_{uu}]\{\ddot{\delta}\} + [C_{uu}]\{\dot{\delta}\} + [[K_{uu}] - [K_{u\phi}][K_{\phi\phi}]^{-1}[K_{\phi u}]]\{\delta\} = \{F_s\} - [K_{u\phi}][K_{\phi\phi}]^{-1}\{F_q\} \tag{4.38}$$

where $[M_{uu}], [K_{uu}], ([K_{u\phi}] = [K_{\phi u}]), [K_{\phi\phi}]$ and $\{F_s\}$ are the corresponding global quantities. $\{\phi_a\}$ is the actuator voltage vector and $[C_{uu}]$ is the structural damping included via Rayleigh damping which is given by,

$$[C_{uu}] = \alpha[M] + \beta[K] \tag{4.39}$$

where α and β are the Rayleigh's constant and $[M]$, $[K]$ effective mass and stiffness matrix.

4.9 Negative velocity feedback and vibration control

In order to provide proper velocity information to the piezoelectric actuators, the voltage induced in the sensor layer is differentiated and fed back. Accordingly, a feedback control gain is used to enhance the sensor signal and also to change its sign before the voltage is injected into the piezoelectric actuators [8].

Constant-gain negative velocity feedback

In this method of control, the sensor signal is differentiated so that strain rate (related to velocity) information is obtained and the actuator voltage is given by

$$\phi_a(t) = -G_c\phi_s(t) \tag{4.40}$$

The velocity feedback can enhance the system damping and therefore effectively control the oscillation amplitude decays the feedback voltage also decreases. This will reduce the effectiveness at low vibration levels for a given voltage unit. In order to provide proper velocity information to the piezoelectric actuators, the voltage induced in the sensor layer is differentiated and fed back. Accordingly, a feedback control gain is used to enhance the sensor signal and also to change its sign before the voltage is injected into the piezoelectric actuators [9].

CHAPTER 5

NEURAL NETWORK

5.1 Introduction

Work on artificial neural networks, commonly referred to as "neural networks," has been motivated right from its inception by the recognition that the human brain computes in an entirely different way from the conventional digital computer. The brain is a highly *complex, nonlinear,* and *parallel computer* (information-processing system). It has the capability to organize its structural constituents, known as neurons, so as to perform certain computations (e.g., pattern recognition, perception, and motor control) many times faster than the fastest digital computer in existence today.

A "developing" neuron is synonymous with a plastic brain: *Plasticity* permits developing nervous system to adapt to its surrounding environment. Just as plasticity appears to be essential to the functioning of neurons as information-processing units in the human brain, so it is with neural networks made up of artificial neurons. In its most general form, a *neural network* is a machine that is designed to *model* the way in which the brain performs a particular task or function of interest; the network is usually implemented by using electronic components or is simulated in software on a digital computer. To achieve good performance, neural networks employ a massive interconnection of simple computing cells referred to as "neurons" or "processing units." We may thus offer the following definition of a neural network viewed as an adaptive machine:

> *A neural network is a massively parallel distributed processor made up of simple processing units, which has a natural propensity for storing experiential knowledge and making it available for use.* It resembles the brain in two respects:
>
> 1. Knowledge is acquired by the network from its environment through a learning process.
> 2. Interneuron connection strengths, known as synaptic weights, are used to store the acquired knowledge.

The procedure used to perform the learning process is called a learning algorithm, the function of which is to modify the synaptic weights of the network in an orderly fashion to attain a desired design objective.

The modification of synaptic weights provides the traditional method for the design of neural networks. Such an approach is the closest to linear adaptive filter theory, which is already well established and successfully applied in many diverse fields. However, it is also possible for a neural network to modify its own topology, which is motivated by the fact that neurons in the human brain can die and that new synaptic connections can grow [11].

5.2 Benefits of Neural Networks

It is apparent that a neural network derives its computing power through, first, its massively parallel distributed structure and, second, its ability to learn and therefore generalize. *Generalization* refers to the neural network producing reasonable outputs for inputs not encountered during training (learning). These two information-processing capabilities make it possible for neural networks to solve complex (large-scale) problems that are currently intractable.

The use of neural networks offers the following useful properties and capabilities:

1. *Nonlinearity.* An artificial neuron can be linear or nonlinear. A neural network, made up of an interconnection of nonlinear neurons, is itself nonlinear. Moreover, the nonlinearity is of a special kind in the sense that it is distributed throughout network.

2. *Input-Output Mapping.* A popular paradigm of learning called learning with a teacher or supervised learning involves modification of the synaptic weights of a neural network by applying a set of labeled *training samples or task examples.* Each example consists of a unique *input signal* and a corresponding *desired response.* The training of the network is repeated for many examples in the set until the network reaches a steady state where there are no further significant changes in the synaptic weights. The previously applied training examples may be reapplied during the training session but in a different order. Thus the network learns from the examples by constructing an *input-output mapping* for the problem at hand.

3. *Adaptivity.* Neural networks have a built-in capability to *adapt* their synaptic weights to changes in the surrounding environment. In particular, a neural network trained to operate in a specific environment can be easily *retrained* to deal with minor changes in the operating environmental conditions. The natural architecture of a neural network for pattern classification, signal processing, and control applications, coupled with the adaptive capability of the network, make it a useful tool in adaptive pattern classification, adaptive signal processing, and adaptive control.

4. *Evidential Response.* In the context of pattern classification, a neural network can be designed to provide information not only about which particular pattern to select, but also about the confidence in the decision made. This latter information may be used to reject ambiguous patterns, should they arise, and thereby improve the classification performance of the network.

5. *Contextual Information.* Knowledge is represented by the very structure and activation state of a neural network. Every neuron in the network is potentially affected by the global activity of all other neurons in the network. Consequently, contextual information is dealt with naturally by a neural network.

6. *Fault Tolerance.* A neural network, implemented in hardware form, has the potential to be inherently *fault tolerant*, or capable of robust computation, in the sense that its performance degrades gracefully under adverse operating conditions. For example, if a neuron or its connecting links are damaged, recall of a stored pattern is impaired in quality. However, due to the distributed nature of information stored in the network, the damage has to be extensive before the overall response of the network is degraded seriously. Thus, in. principle, a neural network exhibits a graceful degradation in performance rather than catastrophic failure [11].

5.3 Model of a Neuron

A neuron is an information-processing unit that is fundamental to the operation of a neural network. The block diagram of Fig.5.1 shows the model of a neuron, which forms the basis for designing (artificial) neural networks. Here we identify three basic elements of the neuronal model [11]:

1. A set of *synapses* or *connecting links*, each of which is characterized by a *weight* or strength of its own. Specifically, a signal x_i at the input of synapse '*i*' connected to neuron '*k*' is multiplied by the synaptic weight w_{ki}. It is important to make a note of the manner in which the subscripts of the synaptic weight w_{ki} are written. The first subscript refers to the neuron in question and the second subscript refers to the input end of the synapse to which the weight refers. Unlike a synapse in the brain, the synaptic weight of an artificial neuron may lie in a range that includes negative as well as positive values.

2. An *adder* for summing the input signals, weighted by the respective synapses of the neuron; the operations described here constitutes a *linear combiner.*

3. An *activation function* for limiting the amplitude of the output of a neuron. The activation function is also referred to as a squashing function in that it squashes (limits) the permissible amplitude range of the output signal to some finite value

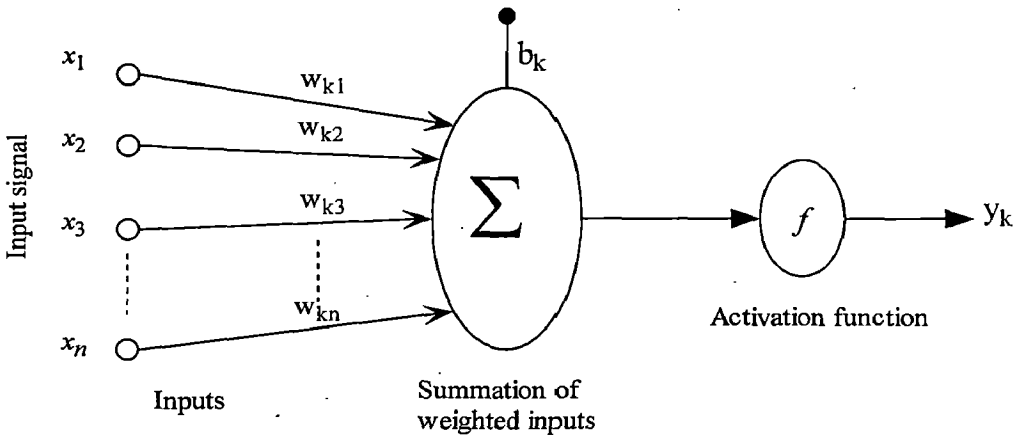

Figure 5.1 Nonlinear model of a neuron [12]

An effective synapse which transmits a stronger signal will have a correspondingly larger weight while a weak synapse will have smaller weights. Thus, weights here are multiplied factors of the inputs to account for the strength of the synapse. Hence, the total input received by the neuron is

$$u_k = w_{k1}x_1 + w_{k2}x_1 + \ldots\ldots + w_{kn}x_n \tag{5.1}$$

$$= \sum_{i=1}^{n} w_{ki}x_i \tag{5.2}$$

and $y_k = f(u_k + b_k) = f(v_k)$ (5.3)

where u_k is the *linear combination output* due to input signals; and b_k is bias; $f(\ )$ is the *activation function*; and y_k is the output signal of the neuron.

5.4 Network Architectures

The manner in which the neurons of a neural network are structured is intimately linked with the learning algorithm used to train the network. In general, there are three fundamentally different classes of network architectures [11].

5.4.1. Single-Layer Feedforward Networks

In a layered neural network the neurons are organized in the form of layers. In the simplest form of a layered network, there is an input layer of source nodes that projects onto an output layer of neurons (computation nodes), but not vice versa. In other words, this network is strictly a. *feedforward* or *acyclic type*. It is illustrated in Fig.5.2 for the case of four nodes in both the input and output layers. Such a network is called a *single-layer network*, with the designation "single-layer" referring to the output layer of computation nodes (neurons). The input layer of source nodes is not counted because no computation is performed there.

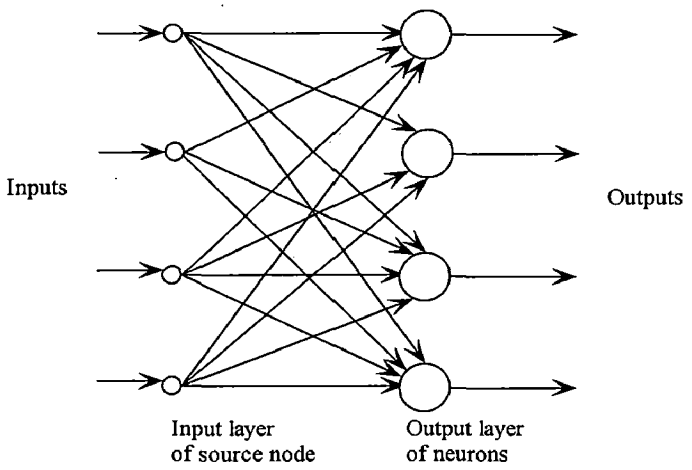

Figure 5.2 Single layer feedback network [11]

5.4.2. Multilayer Feedforward Networks

The second class of a feedforward neural network distinguishes itself by the presence of one or more hidden layers, whose computation nodes are correspondingly called hidden neurons or hidden units. The function of hidden neurons is to intervene between the external input and the network output in some useful manner. By adding one or more hidden layers, the network is enabled to extract higher-order statistics. In a rather loose sense the network acquires a global perspective despite its local connectivity due to the extra set of synaptic connections and the extra dimension of neural interactions. The ability of hidden neurons to extract higher-order statistics is particularly valuable when the size of the input layer is large.

The architectural graph in Fig. 5.3 illustrates the layout of a multilayer feedforward neural network for the case of a single hidden layer.

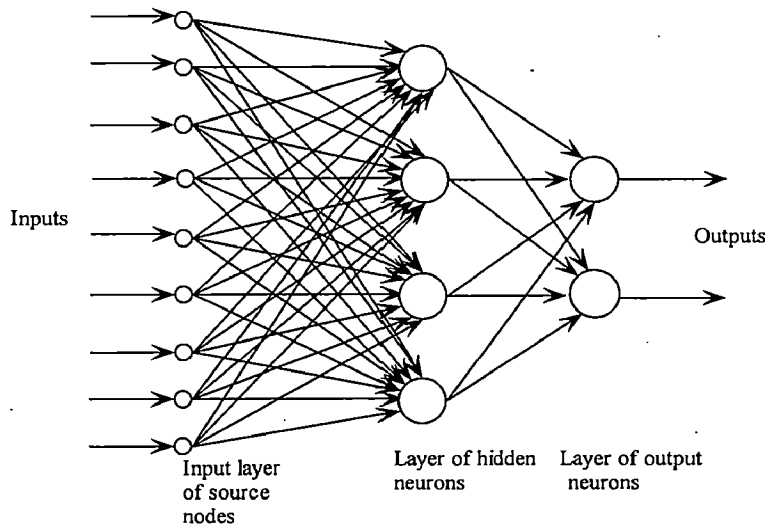

Figure 5.3 Multilayer feedback network [11]

The neural network in Fig. 5.3 is said to be fully connected in the sense that every node in each layer of the network is connected to every other node in the adjacent forward layer. If, however, some of the communication links (synaptic connections) are missing from the network, we say that the network is partially connected.

5.5 Learning Process

Learning is the process by which the free parameters of a neural network are adapted through a process of simulation by the environment in which the network is embedded. The type of learning is determined by the manner in which the parameter changes takes place [11].

Learning methods in Neural Network can be broadly classified into three basic types: *supervised*, *unsupervised*, and *reinforced*.

1. *Supervised learning*. In this learning method, every input pattern that is used to train the network is associated with an output pattern, which is the target or the desired pattern. A teacher is assumed to be present during the learning process, when a comparison is made between the network's computed output and the correct expected output, to determine the error. The error can then be used to change network's parameters, which result in an improved in performance.

2. *Unsupervised learning*. In this learning method, the target output is not presented to the network. It is as if there is no teacher to present the desired patterns and hence, the system learns of its own by discovering and adapting to structural features in the input patterns.

3. *Reinforced learning*. In this method, a teacher though available, does not present the expected answer but only indicates if the computed output is correct or incorrect. The information provided helps the network in its learning process. A reward is given for a correct answer computed and a penalty for a wrong answer [12].

5.6 Training Multilayer Networks

The procedure for selecting the network parameters (weights and biases) for a given problem is called *training* the network [13]. In this section a training procedure described called *backpropagation*. The training process requires a set of examples of proper network behavior - network inputs and target outputs. During training the weights and biases of the network are iteratively adjusted to minimize the network performance function. The default performance function for feedforward networks is *mean square error* (*mse* - the average squared error between the network outputs and the target outputs).

5.6.1 Back propagation Networks

Back propagation is a symmetric method of training multilayer artificial neural networks. It is built on high mathematical foundation and has very good application potential. It is applied to a wide range of practical problems and has successfully demonstrated its power [12].

The training of a Multilayer network is usually accomplished by using a back-propagation. (BP) algorithm that involves two phases

1. *Forward Phase*. During this phase the free parameters of the network are fixed, and the input signal is propagated through the network. The forward phase finishes with the computation of an error signal.

$$e_i = (y_i^d - y_i) \tag{5.4}$$

where y_i^d is the desired output and y_i is the actual output produced by the network in response to the input x_i.

2. *Backward Phase*. During this second phase, the error signal e_i is propagated through the network in the backward direction, hence the name of the algorithm. It is during this phase that adjustments are applied to the free parameters of the network so as to minimize the error in a statistical sense.

5.6.2 Back Propagation Algorithm

The back-propagation algorithm is central to much current work on learning in neural networks. Back-propagation learning may be implemented in one of two basic ways, as summarized here:

1. *Sequential mode* (also referred to as the on-line mode or stochastic mode): In this mode of BP learning, adjustments are made to the free parameters of the network on an example-by example basis. The sequential mode is best suited for pattern classification.

2. *Batch mode*: In this second mode of BP learning, adjustments are made to the free parameters of the network on an epoch by- epoch basis, where each epoch consists of the entire set of training examples. The batch mode is best suited for nonlinear regression [11].

The algorithm gives a prescription for changing the weights w'_{pq} in any feed-forward network to learn a training set of input-output pairs. The network is shown in fig. 5.4 , x is $n\times1$ input vector and y is a $m\times1$ diagonal output vector. The hidden layer consists of h computational units, w'_{ij} represents a typical connection weights between output layer and hidden layer while w'_{jk} represents a typical connection weight between hidden layer and input layer.

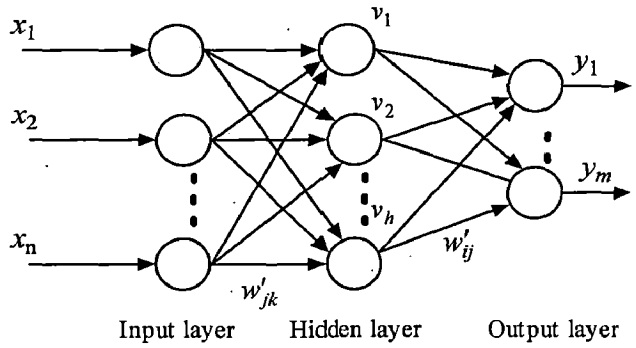

Figure 5.4 A two layered network [11]

Forward Propagation

The forward response of such a network is given as follows:

The input to the j^{th} hidden unit is expressed as

$$S'_j = \sum_{k=1}^{n} w'_{jk} x_k \tag{5.5}$$

Output of the j^{th} hidden unit is given as

$$v_j = f(S'_j) \tag{5.6}$$

where f is the squashing function, generally taken as sigmoidal activation

$$f(x) = \frac{1}{1+e^{-x}} \tag{5.7}$$

Finally the input to the i^{th} output unit is

$$q'_i = \sum_{i=1}^{h} w'_{ij} v_j \tag{5.8}$$

Output y is given as

$$y'_i = f(q'_i) \tag{5.9}$$

Backward Propagation

The instantaneous error back propagation algorithm is derived following the simple gradient principle where, a typical weight w'_{ij} between output layer (j) and hidden layer (i) is updated as follows

$$w'_{ij}(t+1) = w'_{ij}(t) - \eta \frac{\partial E}{\partial w_{ij}} \tag{5.10}$$

where η is the learning rate and $e = \frac{1}{2}(y^d(t) - y(t))^2$ is the error function to be minimized [15].

Algorithm

The implementation of error back-propagation algorithm can be given as follows [15]

1. Initialize the weights to small random values.
2. Choose a pattern x_k k=1, 2,..... n and apply it to the input layer.
3. Propagate the signal forward through the network using

$$S'_j = \sum_{k=1}^{n} w'_{jk} x_k \tag{5.11}$$

$$v'_j = f(S'_j) \quad j = 1,2,.....h \tag{5.12}$$

$$q'_i = \sum_{i=1}^{h} w'_{ij} v_j \tag{5.13}$$

$$y'_i = f(q'_i) \quad i = 1,2,.....n \tag{5.14}$$

4. Compute the details for the output layers

$$\delta'_i = f(q_i)(y_i^d - y_i) \tag{5.15}$$

By comparing the actual outputs y_i with the desired ones y_i^d for the pattern x_k being considered.

5. Compute the details for the hidden layers by propagating the errors backwards

$$\Delta_j = f(S'_j)\sum_{i=1}^{n} w'_{ij}\delta'_i \tag{5.16}$$

6. Use

$$w'_{ij}(t+1) = w'_{ij}(t) + \eta \delta'_i v_j$$
$$w'_{jk}(t+1) = w'_{jk}(t) + \eta \Delta_j x_k \quad (5.17)$$

to update all connections.

7. Go back to step 2 and repeat for the next pattern.

5.7 Steps involved in developing an Artificial Neural Network

A number of issues should be considered before initiation of any network training. Some of the following issues are relevant to BP ANNs while others are applicable to the design of all ANN types [16].

i) Database size and partitioning

Models developed from data generally depend on database size. ANNs, like other empirical models, may be obtained from databases of any size, however generalization of these models to data from outside the model development domain will be adversely affected. Data to be used for training should be sufficiently large to cover the possible known variation in the problem domain. The development of an ANN requires partitioning of the parent database into three subsets: training, test, and validation. The training subset should include all the data belonging to the problem domain and is used in the training phase to update the weights of the network. The test subset is used the learning process to check the network response for untrained data. The data used in the test subset should be distinct from those used in the training. Based on the performance of the ANN on the test subset, the architecture may be and/or more training cycles applied. The portion of the data is the validation subset which should include examples different from those in the other two subsets.

ii) Data preprocessing, balancing, and enrichment

Several preprocessing techniques are usually applied before the data can be used for training to accelerate convergence. Among these are noise removal, reducing input dimensionality, and data transformation, treatment of non-normally distributed data, data inspection, and deletion of outliers. To balance a database, some of the over-represented classes may be removed or extra examples pertaining to the under-represented class

added. Another way is by duplicating the underrepresented input / output examples and adding random noise to their input data.

iii) Data normalization

Normalization (scaling) of data within a uniform range (e.g., 0-1) is essential (i) to prevent larger numbers from overriding smaller ones, and (ii) to prevent premature saturation of hidden nodes, which impedes the learning process.

iv) Input /output representation

Proper data representation also plays a role in the design of a successful ANN, the data inputs and outputs can be continuous, discrete, or a mixture of both. Binary inputs and outputs are very useful in extracting rules from a trained network.

v) Network weight initialization

Initialization of a network involves assigning initial values for the weights (and thresholds) of all connections links. Weights initialization can have an effect on network convergence. Typically, weights and thresholds are initialized uniformly in a relatively small range with zero-mean random numbers.

vi) BP Learning rate (η)

A high learning rate, η, will accelerate training (because of the large step) by changing the weight vector, w, significantly from one cycle to another. However, this may cause the search to oscillate on the error surface and never converge, thus increasing the risk of overshooting a near-optimal w. In contrast, a small learning rate drives the search steadily in the direction of the global minimum, though slowly. A constant learning rate may be utilized throughout the training process.

vii) BP momentum coefficient (μ)

A momentum term is commonly used in weight updating to help the search escape local minima and reduce the likelihood of search instability. A μ accelerates the weight updates when there is a need to reduce η to avoid oscillation. A $\mu > 1.0$ yields excessive contributions of the weight increments of the previous step and may cause instability. Conversely, an extremely small μ leads to slow training.

viii) Transfer function

The transfer (activation) function is necessary to transform the weighted sum of all signals impinging onto a neuron so as to determine its firing intensity. Most applications utilizing BPANNs employ a sigmoid function. Three basic types of activation function are described here [13]

1. *Threshold Function.* A very commonly used Activation function is the *Thresholding function.* In this, sum is compared with a threshold value θ. If the value of v greater than θ, then the output is 1 else it is 0. For this type of activation function, described in fig.5.2 we have

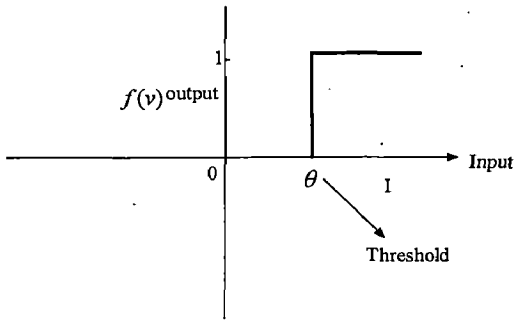

Figure 5.5 Thresholding function [12]

where, v is the step function known as *Heaviside function* and is such that

$$f(v) = \begin{cases} 1, & v > \theta \\ 0, & v \leq \theta \end{cases} \tag{5.18}$$

2. *Signum Function.* Also known as the Quantizer function, the function v is defined as

$$f(v) = \begin{cases} +1, & v > \theta \\ -1, & v \leq \theta \end{cases} \tag{5.19}$$

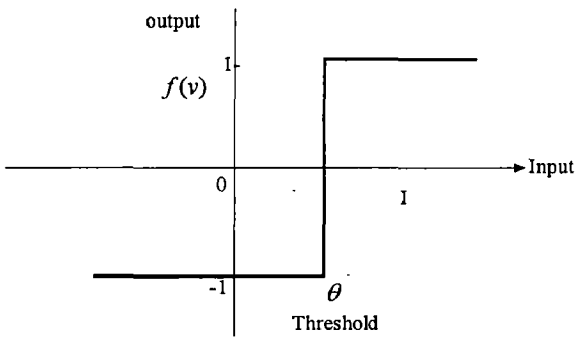

Figure 5.6 Signum function [12]

3. *Sigmoidal Function.* The function is a continuous function that varies gradually between the asymptotic values 0 and 1 or -1 and +1 and is given by

$$f(v) = \frac{1}{1+e^{-\alpha t}} \tag{5.20}$$

where, α is the slope parameter, which adjusts the abruptness of the function as it changes between the two asymptotic values. Fig.5.4 illustrates the sigmoidal function.

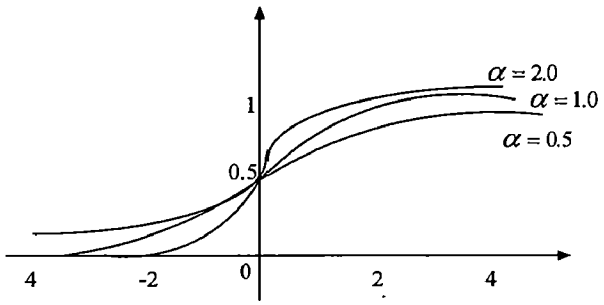

Figure 5.7 Sigmoidal function [12]

ix) Convergence criteria

Three different criteria may be used to stop training: (i) training error (ρ<=ε) (ii) gradient of error (Δρ<=δ), and (iii) cross-validation, where ρ is the arbitrary error function, and ε and δ are small real numbers. The third criterion is more reliable; however it is computationally more demanding and often requires abundant data. Convergence is usually based on the error function, ρ, exhibiting deviation of the predictions from the corresponding target output values such as the sum of squares of deviations. Training proceeds until ρ reduces to minimum. The most commonly used stopping criterion in neural network training is the sum-of-squared-errors (SSE) calculated for the training or test subsets as

$$SSE = \frac{1}{N}\sum_{p=1}^{N}\sum_{i=1}^{M}(t_{pi} - O_{pi})^2 \tag{5.21}$$

where O_{pi} and t_{pi} are, respectively, the actual and target solution of the i^{th} output node on the p^{th} example, N is the number of training examples, M is the number of output nodes. Generally, the error on training data decreases indefinitely with increasing number of hidden nodes or training cycles, as shown in Fig.3.6. The initial large drop in error is due to learning, but the subsequent slow reduction in error may be attributed to (i) network

memorization resulting from the excessively large number of training cycles used, and/or (ii) overfitting due to the use of a large number of hidden nodes. During ANN training, the error on test subsets is monitored which generally shows an initial reduction and a subsequent increase due to memorization and overtraining of the trained ANN.

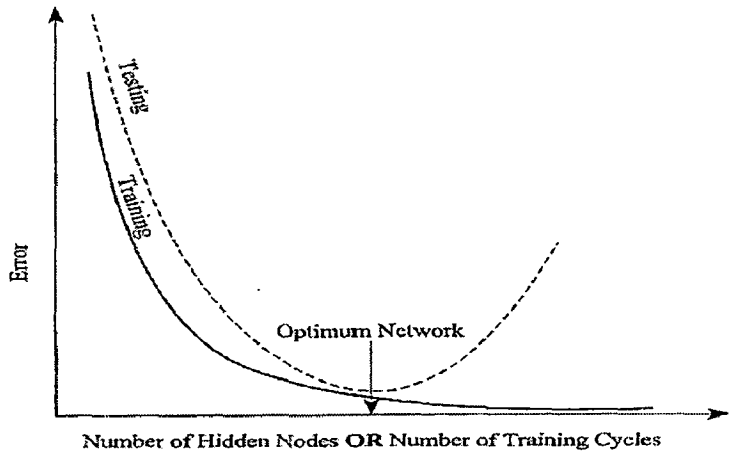

Fig. 5.8 Criteria for termination of training and selection of optimum network architecture [16]

x) Number of training cycles

The number of training cycles required for proper generalization may be determined by trial and error. For a given ANN architecture, the error in both training and test data is monitored for each training cycle. Training for so long can result in a network that can only serve as a look-up table, a phenomenon called overtraining or memorization.

xi) Hidden layer size

In most function approximation problems, one hidden layer is sufficient to approximate continuous functions. The determination of the appropriate number of hidden layers and number of hidden nodes (NHN) in each layer is one of the most critical tasks in ANN design. With increasing number of hidden nodes, training becomes excessively time-consuming. The optimal number of HN essential for network generalization may be a function of input / output vector sizes, size of training and test subsets, and more importantly, the problem of nonlinearity

xii) Parameter optimization

As can be seen, BP training requires a good selection of values of several parameters, commonly through trial and error. Six parameters should not be set too high (large) or too low (small), and thus should be optimized or carefully selected. Table 3.1 lists these parameters and their effect on both learning convergence and overall network performance.

Table 5.1 Effect of extreme values of design parameters on training convergence and network generalization [16]

Design Parameter	Too high or too large	Too low or too small
Number of hidden layers	Over fitting ANN (no generalization)	Under fitting
Learning Rate (η)	Unstable ANN (weights)	Slow Training
Momentum Coefficient (μ)	Reduces risk of local minima. Speeds up training	Entrapment in local minima Slows training
Number of training cycles	Good Recalling ANN	Incapable of responding the data.
Size of training subset	ANN with good generalization	Bad generalization
Size if test sub-set	Ability to confirm ANN generalization capability	Inadequate confirmation of ANN generalization capability

ANNs also have limitations. These include (i) ANNs' success depends on both the quality and quantity of the data, (ii) a lack of physical concepts and relations, and (iii) the inability to explain in a comprehensible form the process through which a given decision (answer) was made by the ANN.

5.8 Neural Network Control

Conventional control theory relies on the key assumption of small range of operation for the linear model to be valid. When the operation range is large, a linear controller is likely to perform poorly or to be unstable, because the nonlinearities in the system cannot be properly compensated for. To implement high-performance control systems when the plant dynamics characteristics are poorly known or when large and unpredictable variations occur, a new class of control systems called nonlinear control systems have evolved which provide potential solutions. Four classes of nonlinear controllers for this purpose are robust controllers, adaptive controllers, fuzzy logic controllers and neural controllers [17].

Complex smart structures, employing a large number of distributed sensors and actuators, are likely to exhibit nonlinearity and variation with time. The classical control requires a high fidelity model of the plant for control law design. Such models, generally based on finite element analysis or experimental identification, are very difficult to obtain for complex structure. Vibration control of smart structure using neural networks has thus been receiving attention for their advantages in self-learning, fault tolerance, and parallel processing [18].

There are typically two steps involved when using neural networks for control

- System Identification
- Control design

System Identification

System identification by neural network is to adjust the connective weights in the multi-layer neural network for minimizing the difference between the network output and desired output by repeated training [15]. Let eq. (5.22) describes the input-output relation of a plant. Then use the set of input-output data's to train a neural network as a model of the system. Let y_i denote the output of the neural network produced in response to an input vector x_i.

$$y_i^d = f(x_i) \tag{5.22}$$

The difference between y_i^d and network output y_i provides the error signal vector e_i, as depicted in fig.5.9. This error signal is in turn used to adjust the free parameters of the network to minimize the squared difference between the outputs of the unknown system and the neural network in a statistical sense, and is computed over the entire training set [11].

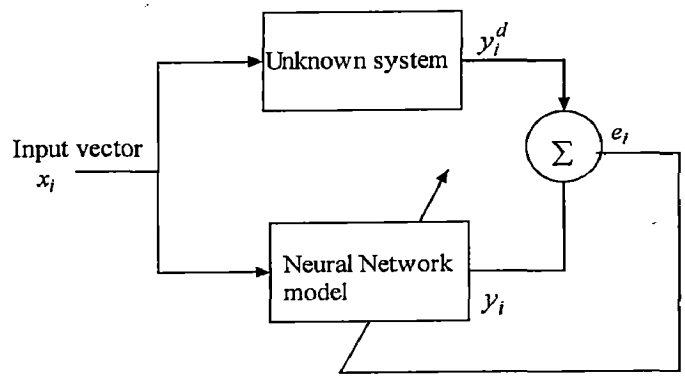

Figure 5.9 Block diagram of system identification [11]

Control design

In a general sense, the identified neuro model is then used to adapt the neural network based controller such that the plant output follows the output of a predetermined reference model. Some of the more popular neural network architectures for system identification and control are described below [13].

5.8.1 Fixed Stabilizing Controller

This type of controller is used for control of robot trajectory, where a proportional controller with gain was used as the stabilizing feedback controller. The advantage of this architecture is that it can start with stable system, even though the neural network has not been adequately trained.

5.8.2 Adaptive Inverse Control

The adaptive algorithm receives the error between the plant output and reference model output. The controller parameters are updated to minimize that tracking error. The basic model reference adaptive control approach can be affected by sensor noise and plant disturbances. An alternative which allows cancellation of the noise and disturbances includes a neural network plant model in parallel with the plant. That model will be

trained to receive the same inputs as the plant and to produce the same output. The difference between the outputs will be interpreted as the effect of noise and disturbances at the plant output. The signal will enter an inverse model to generate a filtered noise and disturbance signal that subtracted from the plant input. The idea is to cancel the disturbance and the noise present in the plant.

5.8.3 Nonlinear Internal Model Control

It consists of neural network controller, a neural network plant model, and a robustness filter with a single tuning parameter. The neural network controller is generally trained to represent the inverse of the plant, if the inverse exists. The error between the output of the neural network plant model and the measurement of the plant output is used as the feedback input to the robustness filter, which then feeds in to the neural network controller.

5.8.4 Model Predictive Control

It optimizes the plant responses over a specified time horizon. This architecture requires a neural network plant model, a neural network controller, a performance function to evaluate system responses, and an optimization procedure to select the best control input. The neural network controller is learns to produce the input selected by the optimization process. When training is complete, the optimization step can be completely replaced by the neural network controller.

5.8.5 Stable Direct Adaptive Control

The method uses Lyapunov stability theory in the design of the network learning rule, rather than a gradient descent algorithm like backpropagation. The controller consists of three parts; linear feedback, a nonlinear sliding mode controller and an adaptive neural network controller. The sliding mode controller is used to keep the system state in a region where the neural network can be accurately trained to achieve optimal control. The sliding mode controller is turned on whenever the system drifts outside this region. The combination of these controllers produces a stable system which adapts to optimize performance.

5.8.6 Modal Reference Control

The Modal Reference Control uses two neural networks; a controller network and a model network. The model network can be trained off-line using historical plant measurements. Then the controller is so that the plant output follows the reference model output. Both model network and controller network are trained using *backpropagation algorithm*. The fig.5.9 shows Modal Reference Control.

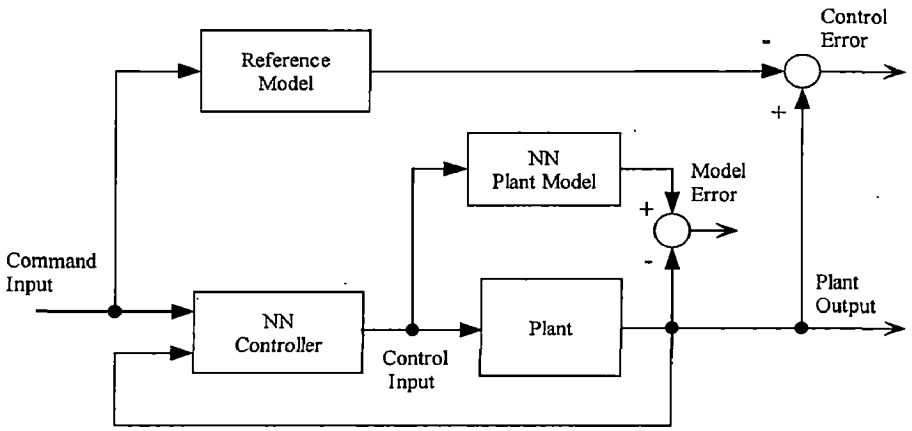

Figure 5.10 Model Reference Control [13]

This control architecture requires the use of dynamic backpropagation for training the controller. This generally takes more time than training static networks with the standard backpropagation algorithm. The controller requires minimal online computation.

5.9 Tapped delay line (TDL)

TDL is used to give the delayed inputs to the network. The number of delays increases with the order of the plant. Fig. 5.7 shows the representation of the TDL.

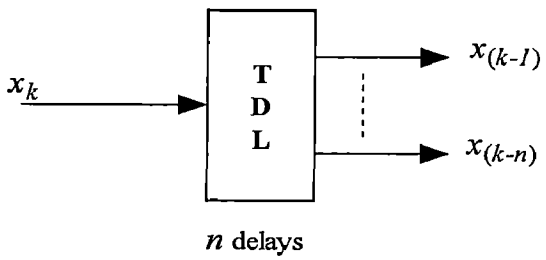

Figure 5.7 TDL

where x_k is the input at k^{th} time instant and $x_{(k-1)}$ and $x_{(k-n)}$ are the inputs at $(k-1)^{th}$ and $(k-n)^{th}$ time instant respectively.

CHAPTER 6

RESULTS AND DISCUSSION

6.1 Validation of the FEM model

The theoretical formulation of the beam model is first validated by comparing obtained numerical results with the experimental and numerical results of other researchers and then provides some new results.

6.1.1 FEM validation without piezolayers

The non-dimensional fundamental frequency for simply supported laminated composite cylindrical panel having dimensions and properties given in the literature [21] is obtained by varying the thickness to radius ratio. The results obtained by present FEM model is compared with the literature [21]. It is observed that both results compare extremely well.

Table 6.1 Non-dimensional fundamental frequencies for simply supported laminated composite cylindrical panel

h/R	Non-dimensional fundamental frequencies ($0^o/90^o$)	
	Reddy	Present FEM
1/300	24.576	25.05
1/400	19.509	19.75
1/500	16.668	16.73

6.1.2 FEM validation with piezolayers

- **Static Validation**

A piezoelectric bimorph cantilever beam *(100mm× 5mm× 1mm)* constructed of two layers of PVDF bonded together with opposite polarity is considered. The beam is modeled with the present FEM. The cantilever is modeled by taking five elements and the deflection of the free end of the beam is compared with [22]. The comparison is shown in Table 6.2.The results agree very well with the theoretical results.

Table 6.2 Nodal deflection of the piezoelectric bimorph beam

Distance (mm)	Deflection(micron)					
	Theory	Beam FEM	QUAD4	Experiment	Shell9	Present FEM
20	0.0138	0.0124	0.0139	-	0.0144	0.0136
40	0.0552	0.0508	0.0547	-	0.557	0.0550
60	0.1242	0.116	0.1135	-	0.1240	0.1239
80	0.2208	0.210	0.2198	-	0.2192	0.2207
100	0.3450	0.330	0.3416	0.315	0.3415	0.3451

- **Dynamic Validation**

A semicircular steel shell embedded with a PZT piezoceramic layers on the top and a bottom surface is considered as shown in fig.6.1 One end of steel ring is fixed and the other end is free. It is 250 mm wide and 5 mm thick with an inner radius of 250 mm. The thickness of the PZT layers are 0.25 mm. The material properties are described in the Table 6.3. The first six natural frequencies are obtained by using present FEM model and are compared with the literature [9]. The comparison is shown in Table 6.4.The results agree very well with the results given in the literature [9].

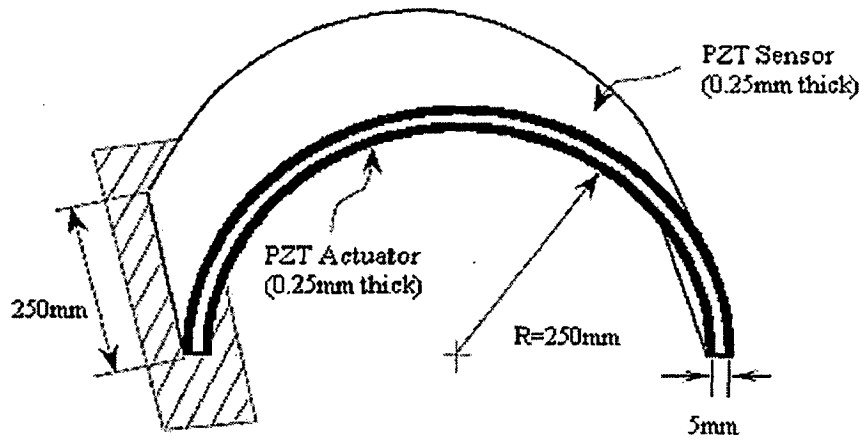

Figure 6.1 Semicircular piezolaminated steel curved beam

Table 6.3 Material properties

Properties	Steel	PZT ceramics
Young's Modulus ($N.m^{-2}$)	$E_1 = E_2 = 210 \times 10^{11}$	$E_a = E_s = 63 \times 10^9$
Density (kg/m^3)	7800	7600
Poisson ratio	$\nu_{12} = 0.3$	$\nu_a = \nu_s = 0.3$
Piezoelectric Constant (m/V)	-	$d_{31} = d_{32} = -1.79 \times 10^{-10}$
Electrical permittivity (F/m)	-	$b_{11} = b_{22} = b_{33} = 1.505 \times 10^{-8}$

Table 6.4 Comparison of Natural frequencies in Hz

Sr.no.	First six natural frequencies by literature [9]	First six natural frequencies by present model
1.	8.61	8.4
2.	14.85	12.10
3.	27.22	26.59
4.	63.19	52.09
5.	93.16	91.61
6.	207.88	206.52

6.2 Case study

A layered curved beam is considered. The top and bottom layers are made of piezoelectric material and middle layer is made of steel. The piezoelectric material is lead-zirconate-titanate (PZT).The radius of curved beam is 0.2 m, width 50 mm, thickness is 3 mm and curvature angle180^0 .The thickness of each piezolayers is 0.25 mm. Detailed material properties are listed in Table 6.5.

Table 6.5 Material properties

Properties	Steel	PZT G1195N ceramics
Young's Modulus	$E_1 = E_2 = 210 \times 10^{11}$ $N.m^{-2}$	$E_1 = E_2 = 63 \times 10^9$ $N.m^{-2}$
Density	7800 Kg/m^3	7600 Kg/m^3
Poisson ratio	$\nu_{12} = 0.3$	$\nu_{12} = 0.3$
Piezoelectric Constant	-	$d_{31} = 2.54 \times 10^{-10}$ (m/V)
Electrical permittivity	-	$b_{33} = 1.505 \times 10^{-8}$ (F/m)

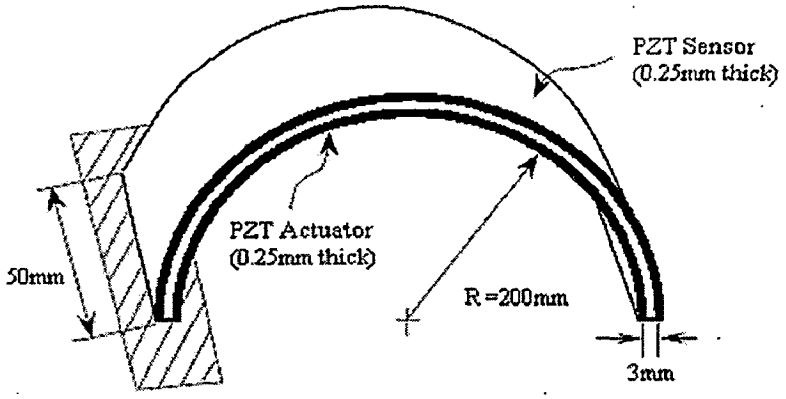

Figure 6.2 Semicircular piezolaminated steel curved beam with one end fixed

6.2.1 Effect of radius of curvature on tip deflection for both symmetric and antisymmetric ply orientation

In this case the total number of layers considered here are four. A point load of 2N is acting on the tip at the free end of the beam. The effect of radius of curvature on tip deflection in case of antisymmetric and symmetric ply orientation in layered beam is presented in table 6.

Total number of layers = 4, no. of piezolayers= 2, F= 2 N

Table 6.6 Effect of radius of curvature on tip deflection

Radius of curvature R (mm)	Tip Deflection (m)	
	Antisymmetric (0°/45°/0°/45°)	Symmetric (0°/45°/45°/0°)
100	1.7599×10^{-5}	2.0418×10^{-5}
150	5.7318×10^{-5}	6.6953×10^{-5}
200	0.000136	0.000160
250	0.000266	0.000311
300	0.000460	0.000540

From Table 6.6 it is observed that for both symmetric and antisymmetric configuration of layered beam a tip deflection increases as radius of curvature increases. For the same radius of curvature tip deflection for symmetric case is more than antisymmetric case.

6.2.2 Shape control of composite curved beam

In fig.6.3 AB is the neural plane of the curved beam. AC shows the deformed position of the neutral plane under tip point load 3 N. To maintain the original position of the neutral plane, electric voltage is applied across the thickness of piezoelectric layers in biomorphic arrangement. For the applied voltages the position of the neutral plane changes as shown in the fig.6.3 and fig.6.4 for curvature angle 90^0 and 180^0 respectively.

a. Shape control for curvature angle of 90^0

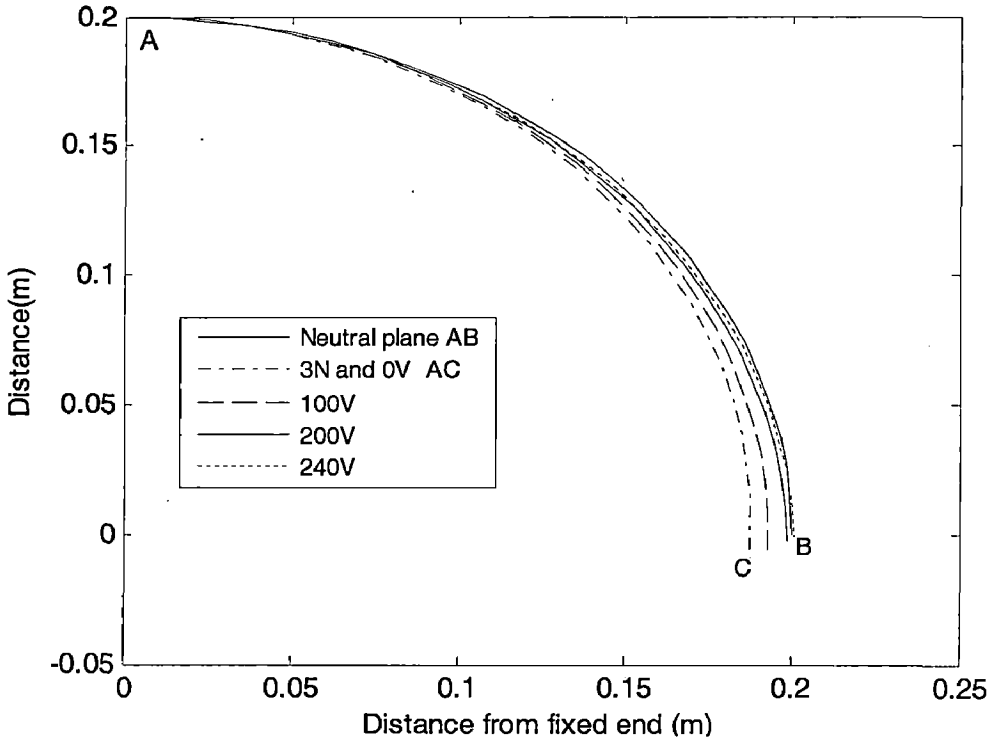

Figure 6.3

Fig. 6.3 shows that applied voltage 100V, 200V, 240V changes the position of the neutral plane. It is observed that neutral plane regains approximate its undeformed position at 240V.

b. Shape control for curvature angle180^0

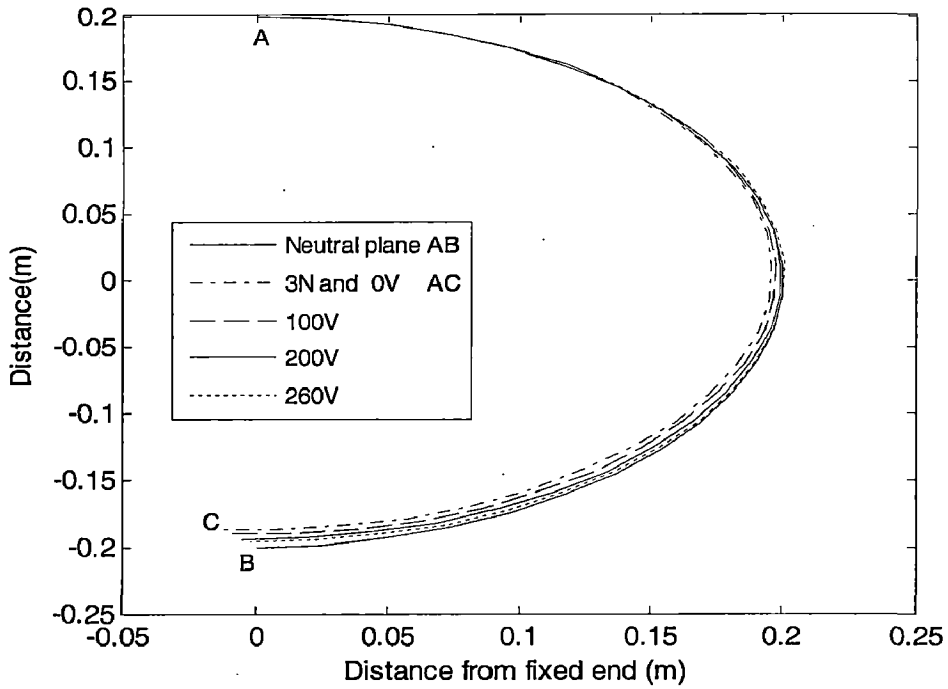

Figure 6.4

Fig. 6.4 shows that the applied voltage 100V, 200V, 260V changes the position of the neutral plane. It is observed that neutral plane regains approximate its undeformed position at 260V.

6.2.3 Tip deflection versus area covered by PZT for different values of radius of curvature

The effect on tip deflection for different values of radius of curvature and for different percentage of actuator coverage area from fixed and free end of the beam is shown in fig.6.5(a) and (b) and fig.6.6 (a), (b), (c) and (d) for curvature angle of 90° respectively.

6.2.3.1 For curvature angle of 90°

a. Actuator coverage area from fixed end

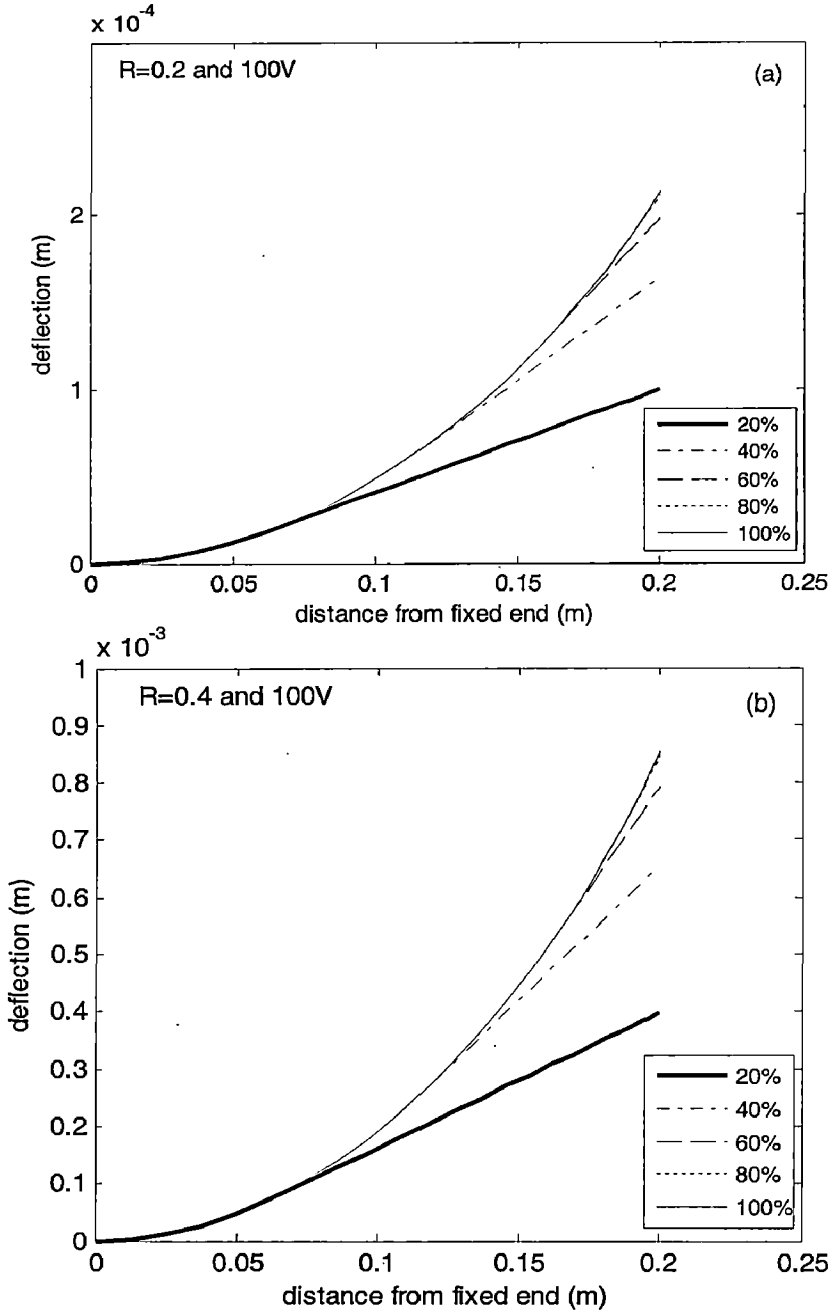

Figure 6.5

From fig.6.5 (a) and (b) it is observed that as the actuator coverage area increases from fixed end the deflection increases at a point which is at distance from fixed end for the given radius of curvature and applied voltage.

b. Actuator coverage area from free end

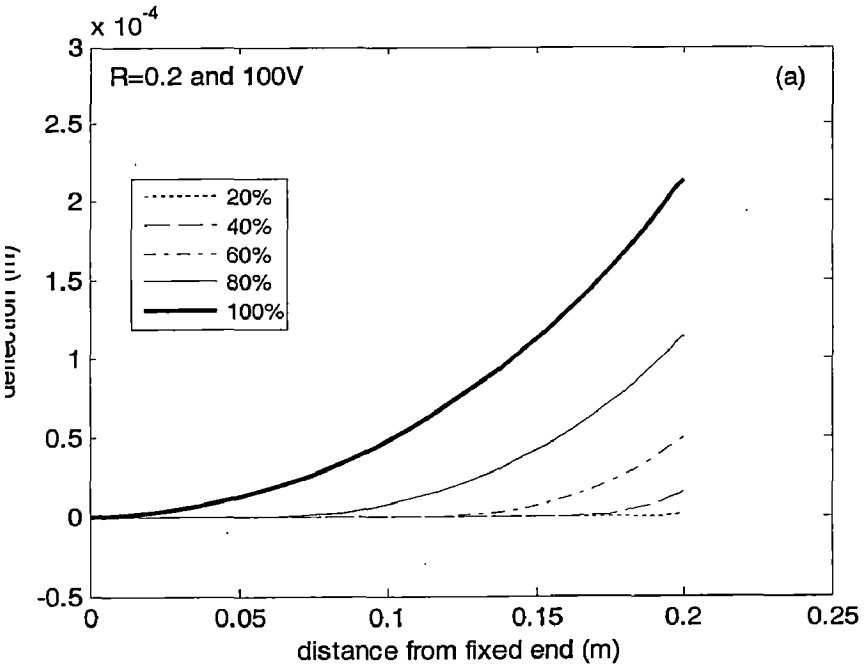

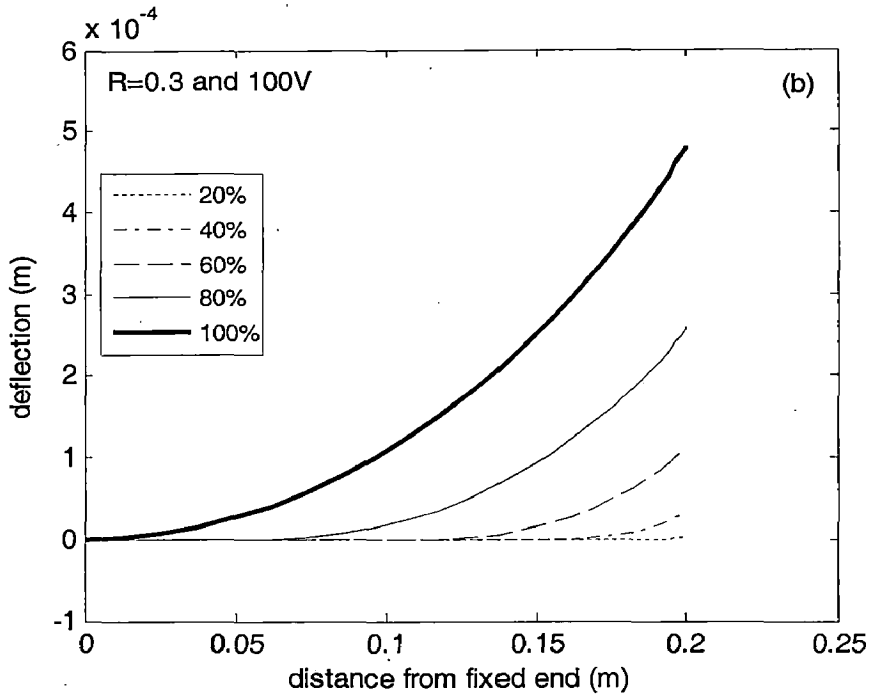

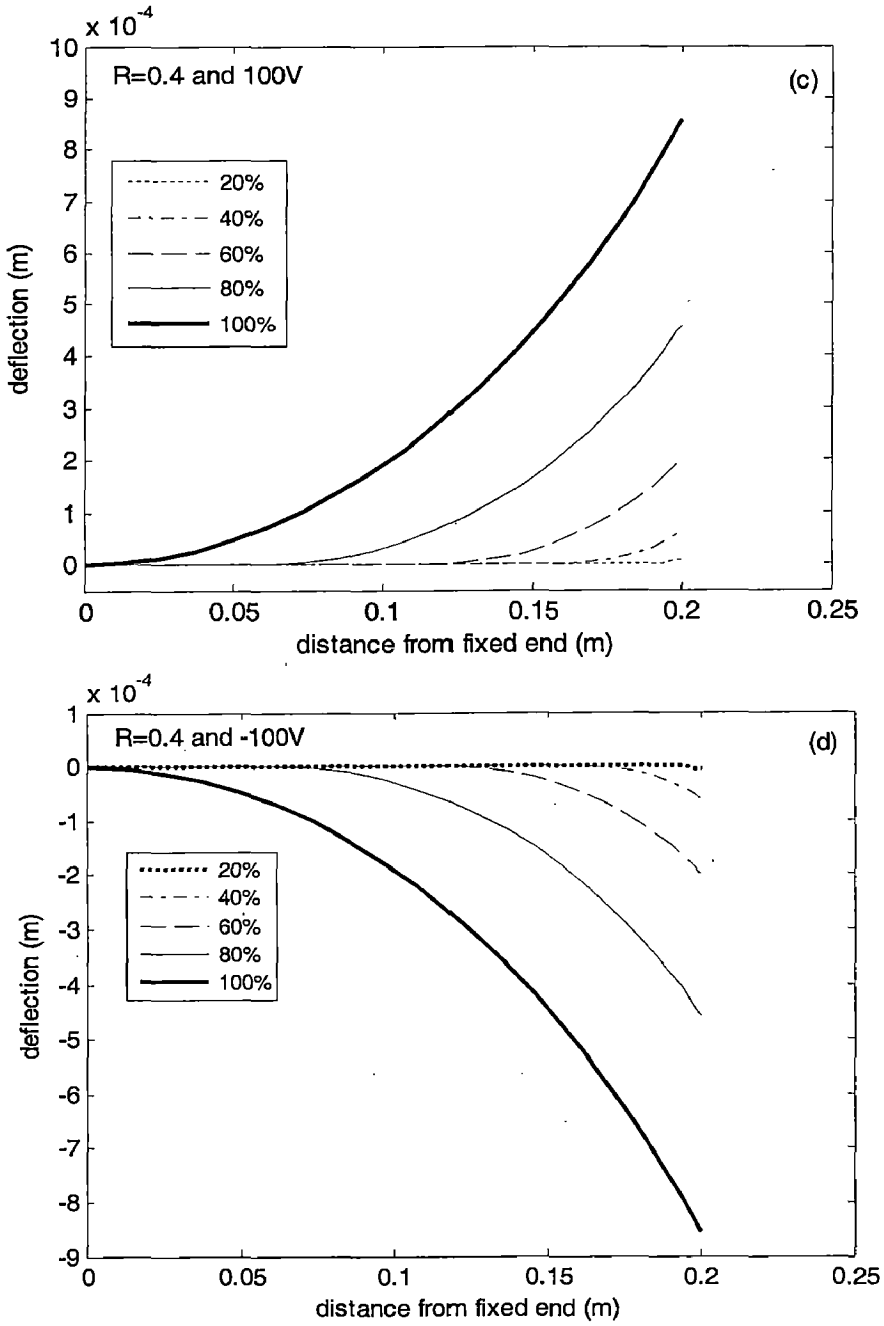

Figure 6.6

From fig.6.6 (a), (b) and (c) it is observed that for the increase in actuator coverage areas from the free end the deflection increases at a point which is at distance from fixed end for given radius of curvature and applied voltage. It is also true for the fig. 6.6 (d) but only deflection is in opposite direction due to opposite polarity voltage. Also for fig 6.6 (c) and (d) have the same value of maximum deflection but in opposite direction.

6.2.3.2 For curvature angle 180° and actuator coverage area from fixed end

The effect on tip deflection for different values of radius of curvature and for different percentage of actuator coverage area from fixed end of the beam is shown in fig.6.7 (a) and (b) for curvature angle of 180°.

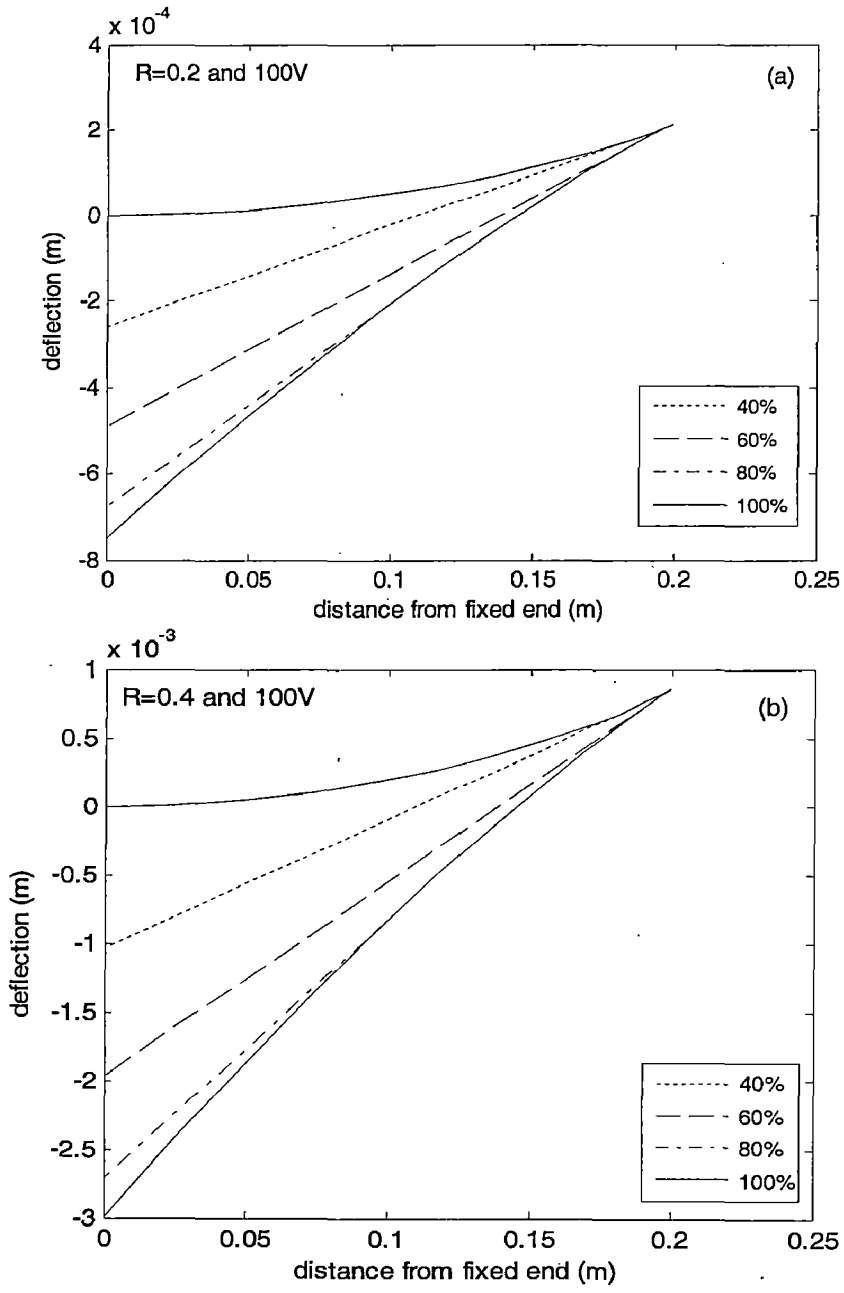

Figure 6.7

6.2.4 Effect of radius of curvature on natural frequency for both symmetric and anti symmetric ply orientation

The effect of radius of curvature on the natural frequency is obtained for antisymmetric and symmetric ply orientation in composite curved beam for curvature angle of 180°.The comparison is shown in the Table 6.7.

Table 6.7 Effect of radius of curvature on natural frequency

Radius of curvature R (mm)	Antisymmetric 0°/45°/0°/45° f (Hz)	Symmetric 0°/45°/45°/0° f (Hz)
100	60	56.22
150	26.54	24.699
200	14.88	13.81
250	9.50	8.8112
300	6.593	6.106

It shows that natural frequency is more in case of antisymmetric composite curved beam compared to symmetric curved beam for the same value of radius of curvature and as the radius of curvature increase natural frequency for both symmetric and antisymmetric layered beam is decreases.

6.2.5 Transient vibration control for different gains

Newmark's direct time integration scheme is adopted to evaluate the transient responses. The values of time integration scheme parameters δ' and α' are assumed 0.5 and 0.25 respectively. We have studied following cases for transient vibration control.

6.2.5.1 For initial displacement of 1mm in hoop direction at free end

An initial displacement of 1mm is applied in the hoop direction and corresponding responses in radial and hoop direction is studied. Fig. 6.8 shows the free vibration response in hoop and radial direction.

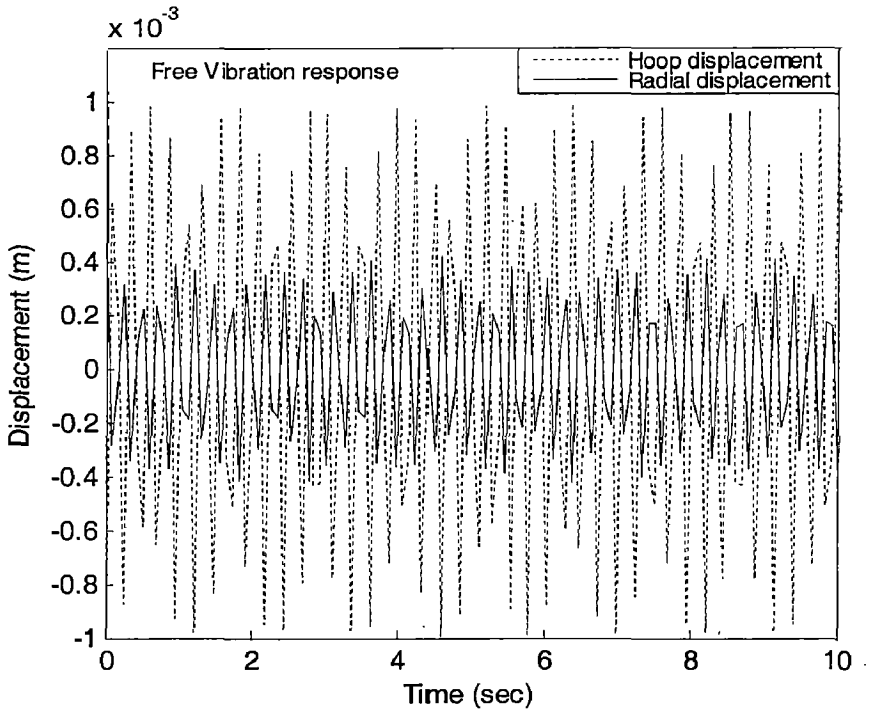

Figure 6.8

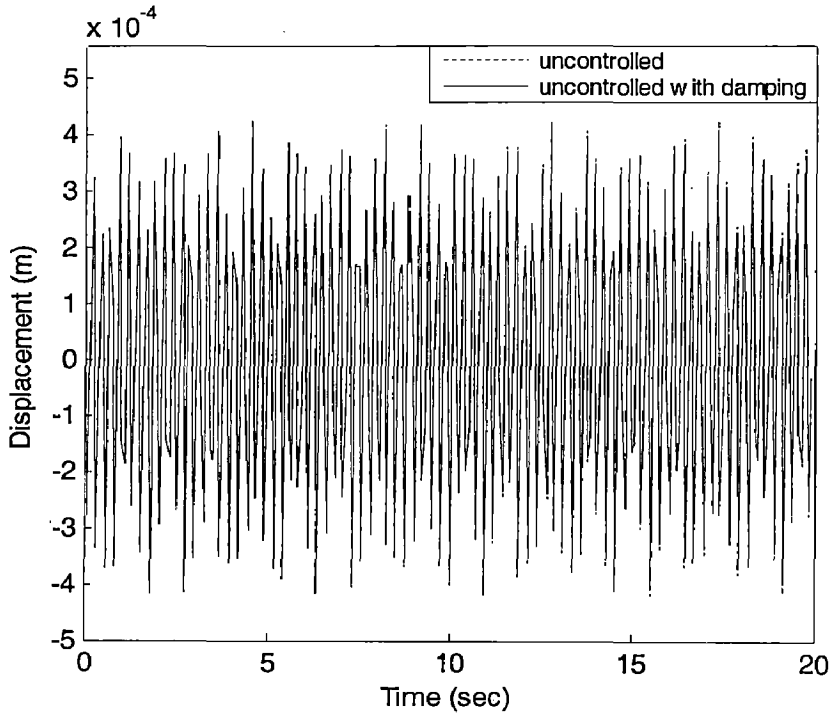

Figure. 6.9

Fig.6.9 shows the effect of passive damping on the free vibration of the beam for the value of damping factor 0.01. It is observed that damping has less effect on vibration decay.

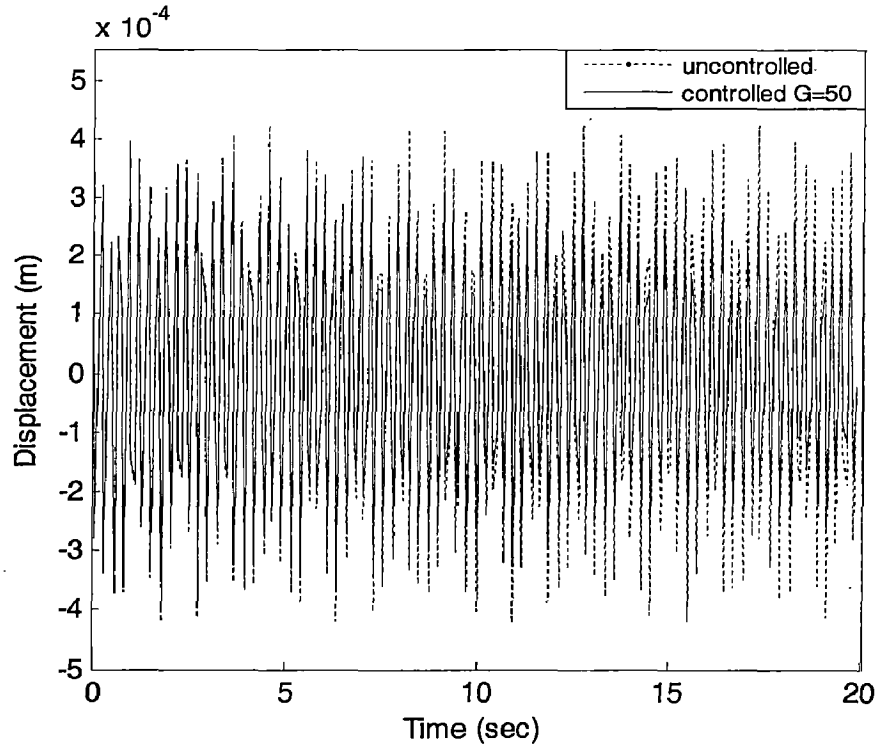

Figure 6.10 (a)

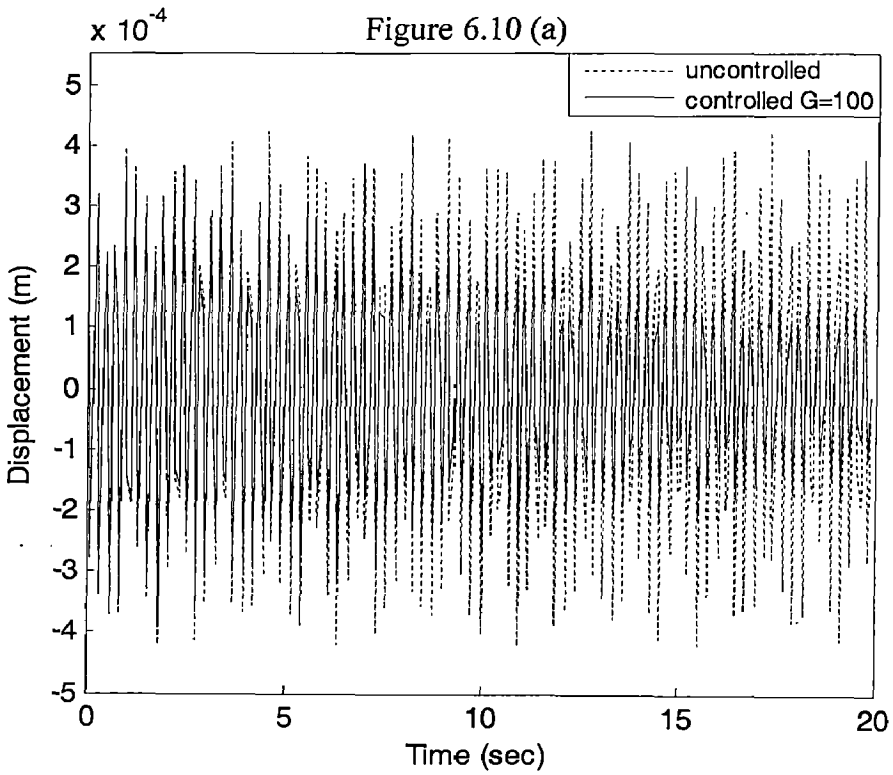

Figure 6.10 (b)

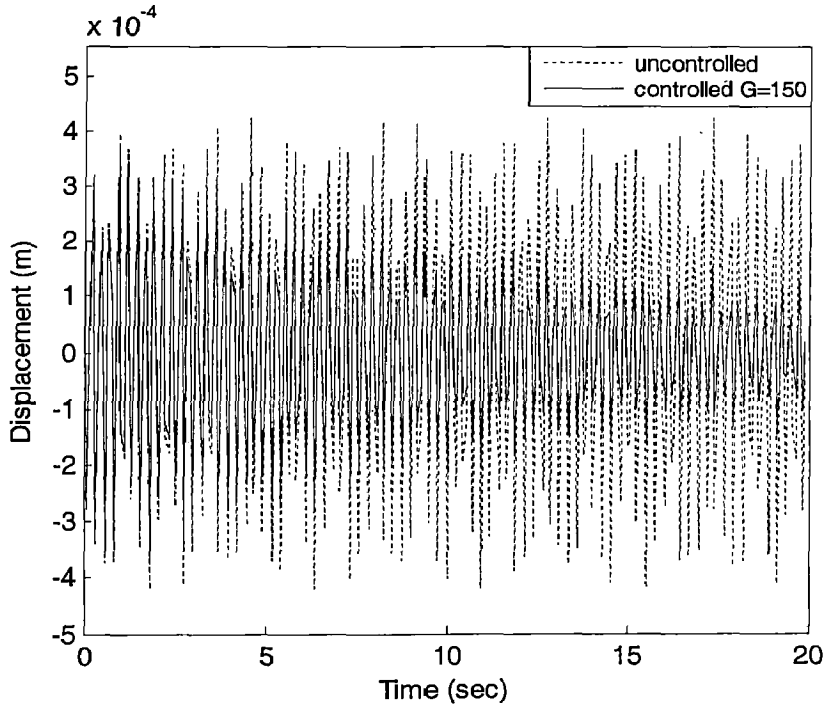

Figure 6.10 (c)

Fig. 6.10 (a), (b) and (c) shows the controlled response in radial direction at gain 50, 100, 150 respectively. It is observed that as gain increases vibration decay lost.

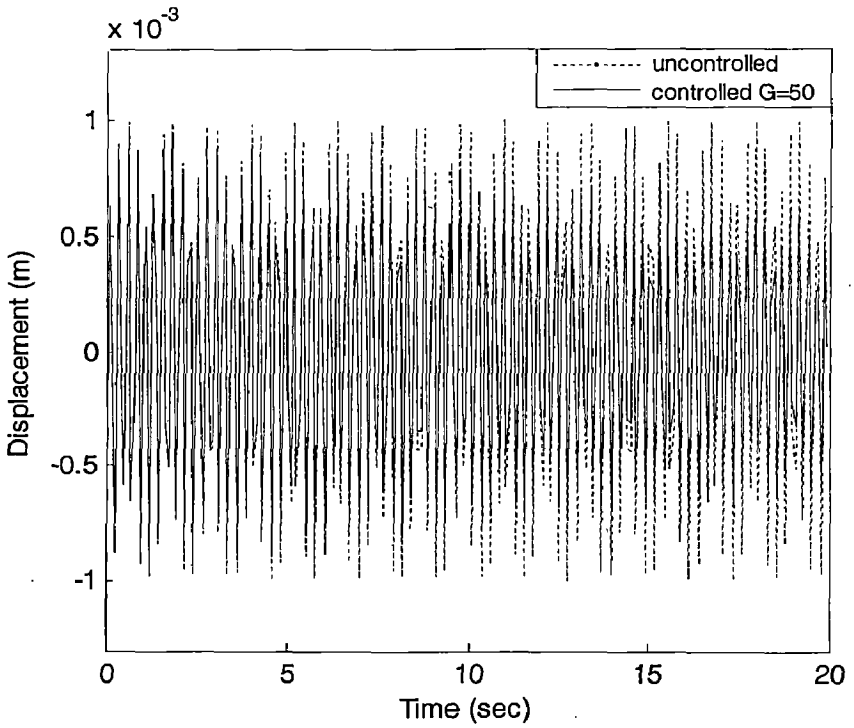

Figure 6.11 (a)

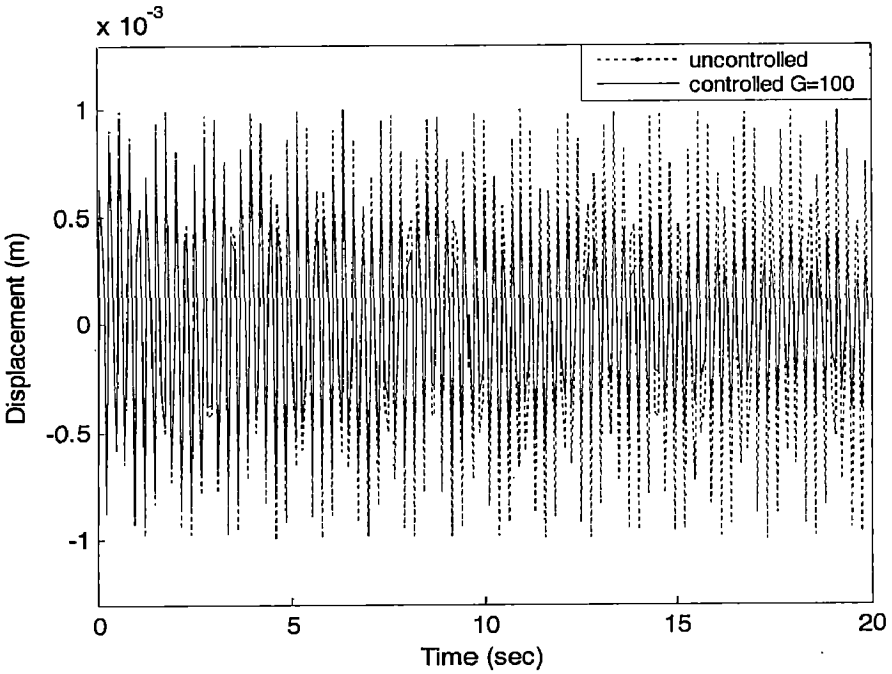

Figure 6.11 (b)

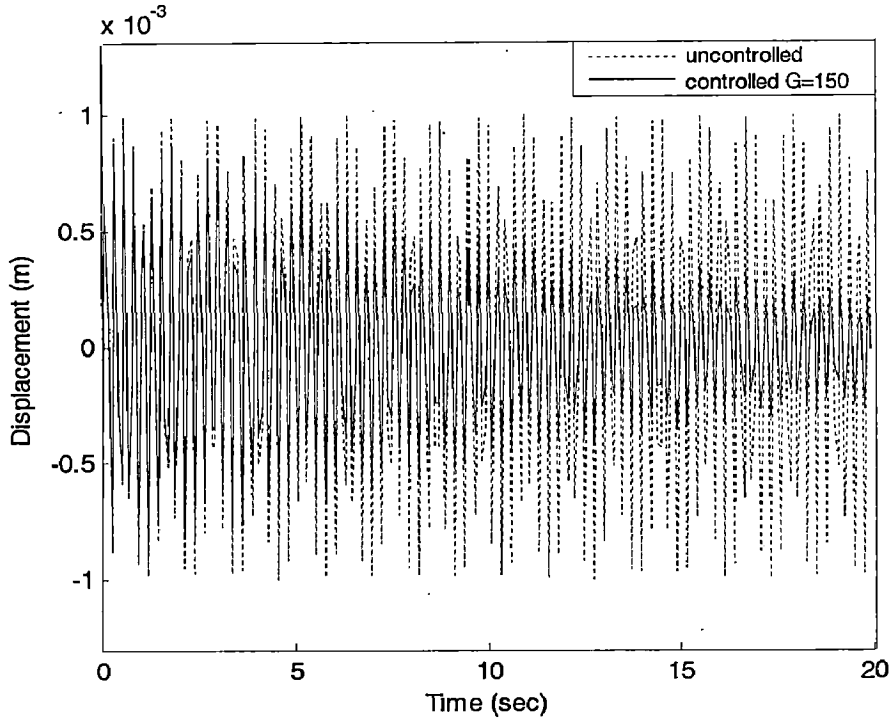

Figure 6.11 (c)

Fig. 6.11 (a), (b) and (c) shows the controlled response in hoop direction at gain 50, 100, 150 respectively. It is observed that as gain increases vibration decay lost.

6.2.5.1 For uniform distributed load

A uniform distributed load of 1000 N/m^2 is applied in the radial direction and corresponding response in radial direction at tip node of composite curved beam is studied. Fig.6.12 shows the uncontrolled response with and without damping.

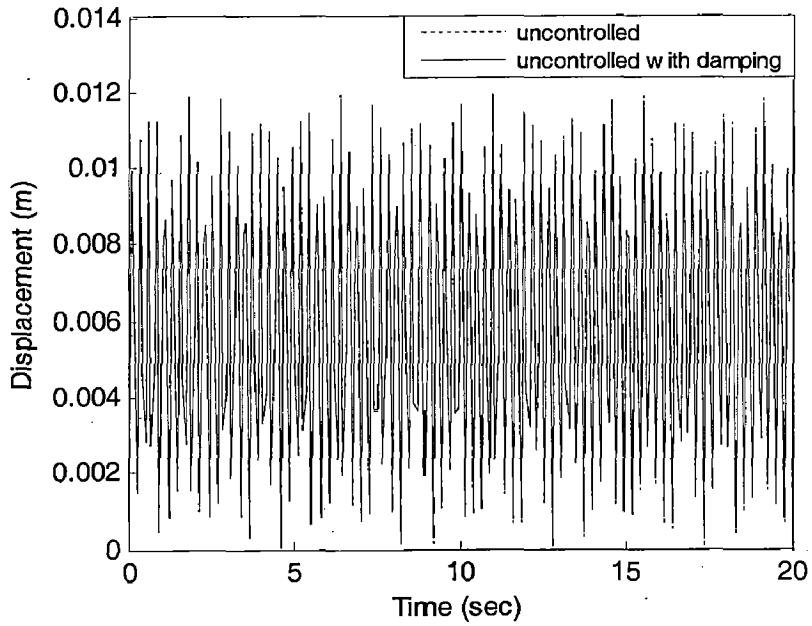

Figure 6.12

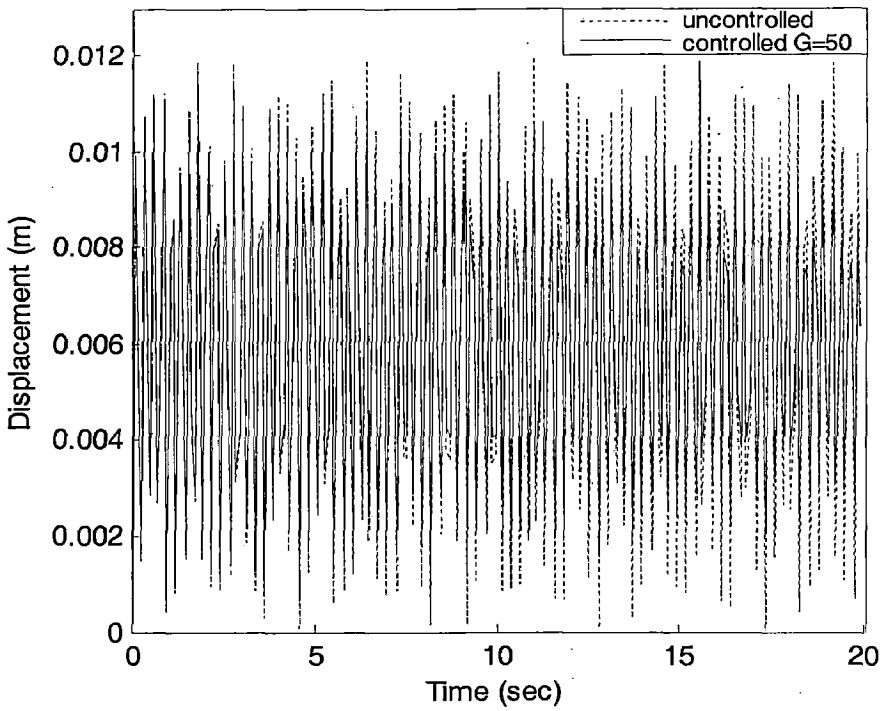

Figure 6.13 (a)

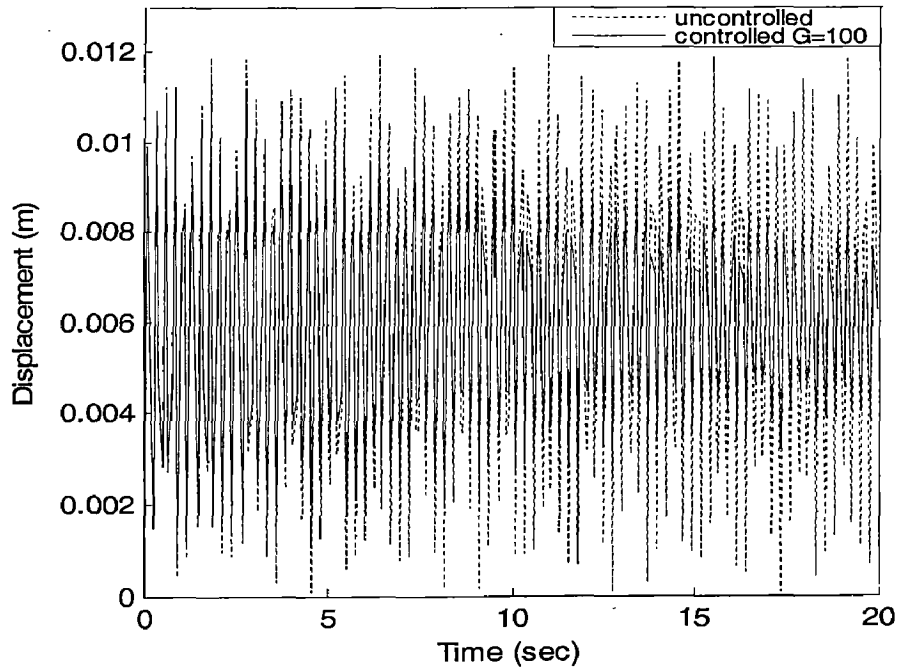

Figure 6.13 (b)

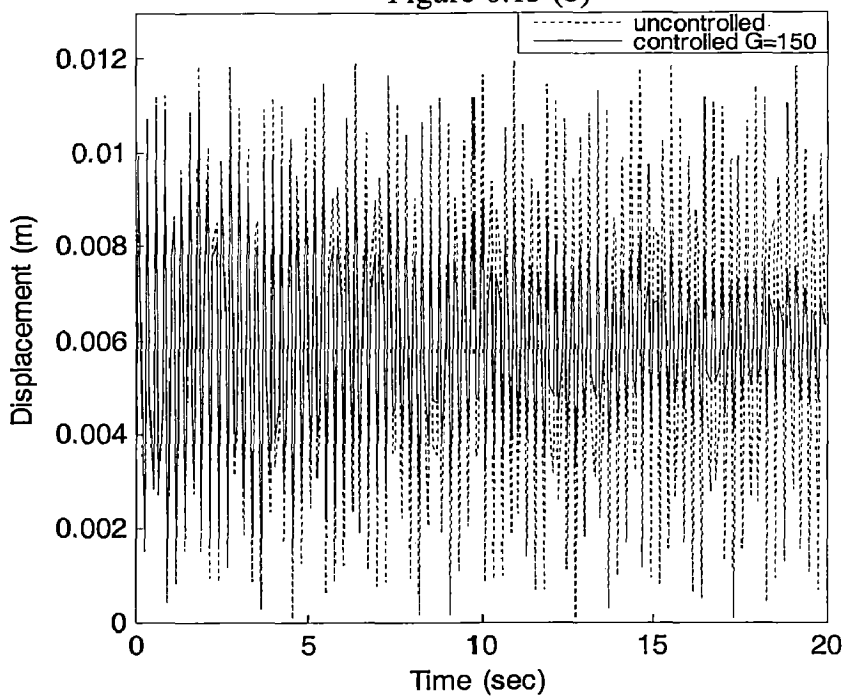

Figure 6.13 (c)

From graph 6.13 (a), (b) & (c) it is clear that as gain increases the control on vibration is effective.

6.2.5.3 Tip Deflection control for initial displacement of 1mm in hoop direction for different piezoelectric layer coverage area

The vibration control of smart composite curved beam is also studied by varying the sensor/actuator percentage coverage area from the free end of the beam for a specific gain.

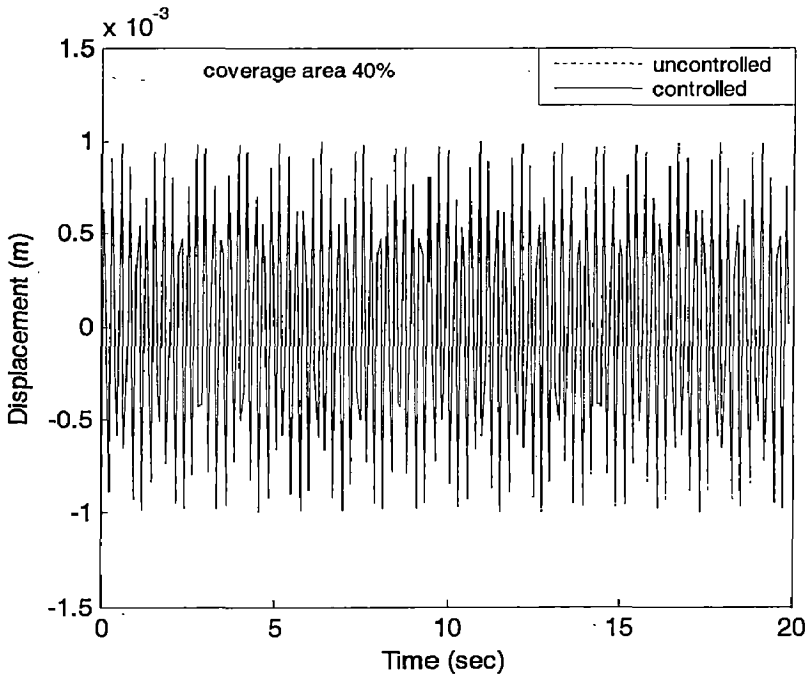

Figure 6.14 (a)

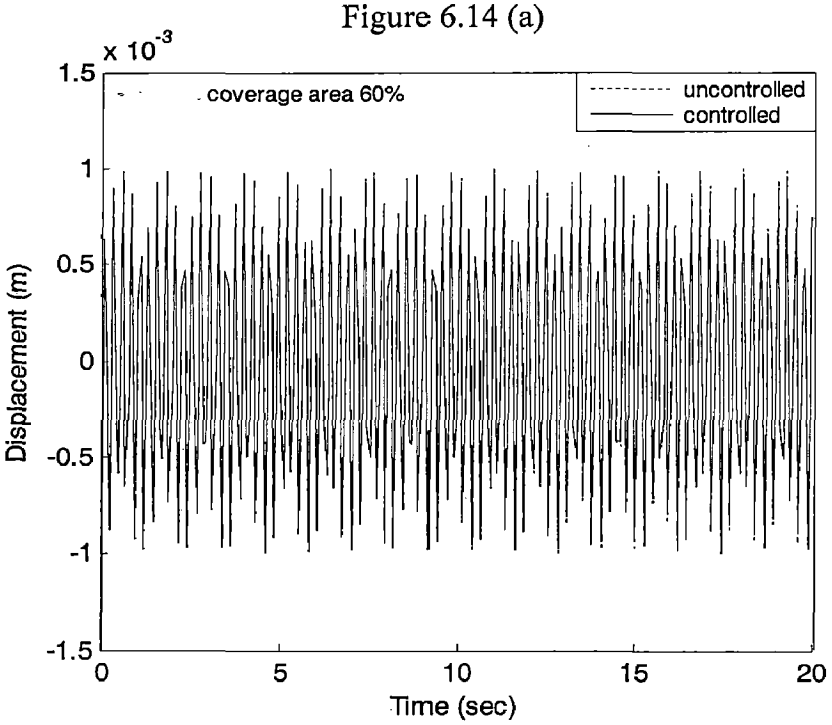

Figure 6.14 (b)

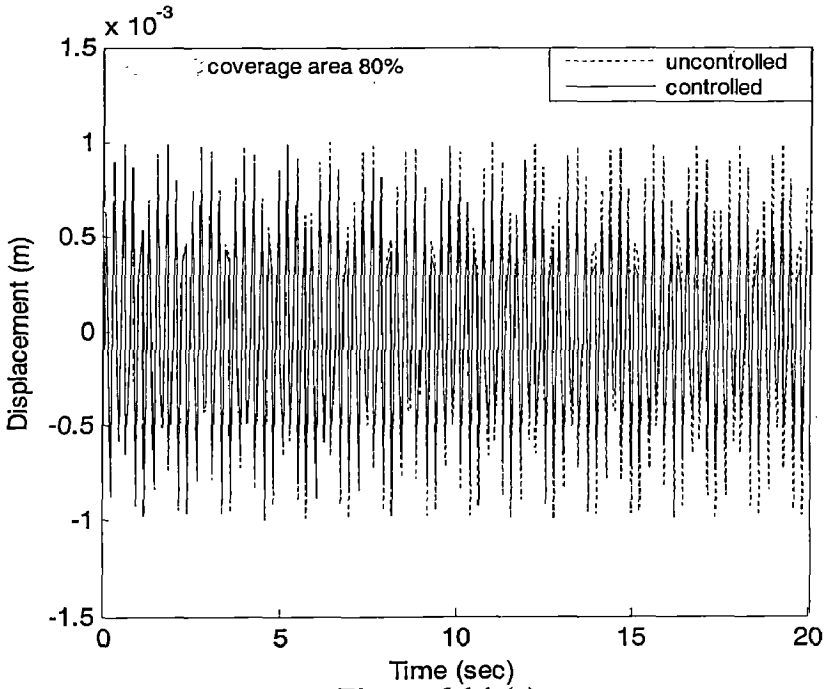

Figure 6.14 (c)

Fig.6.14 (a), (b) and (c) shows the tip responses in hoop direction at 40%, 60% and 80% of piezoelectric layer coverage area from free end respectively for a specific gain G=150. It is observed that vibration decay fast for more coverage area of piezoelectric layer.

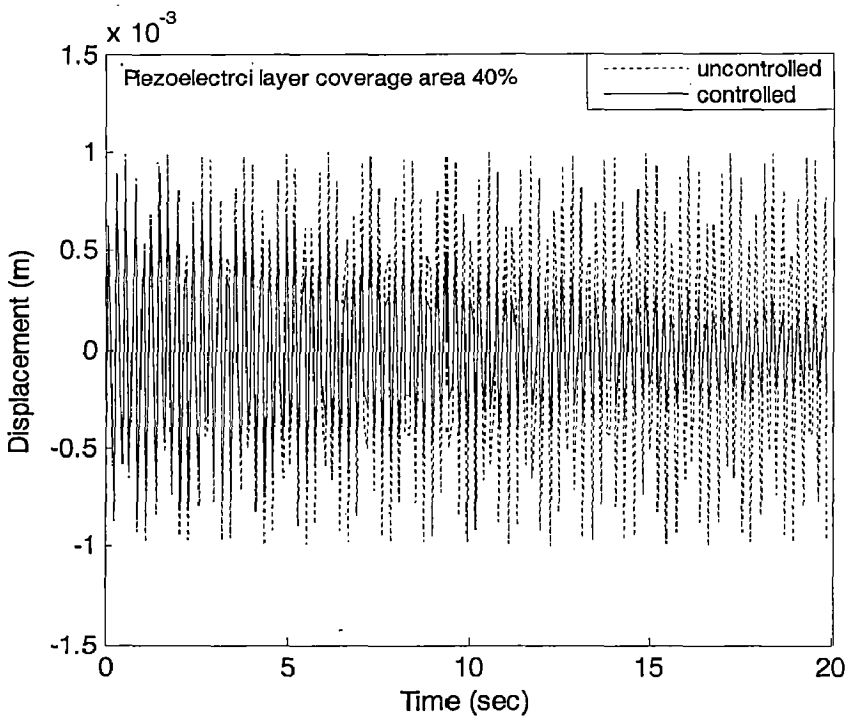

Figure 6.15 (a)

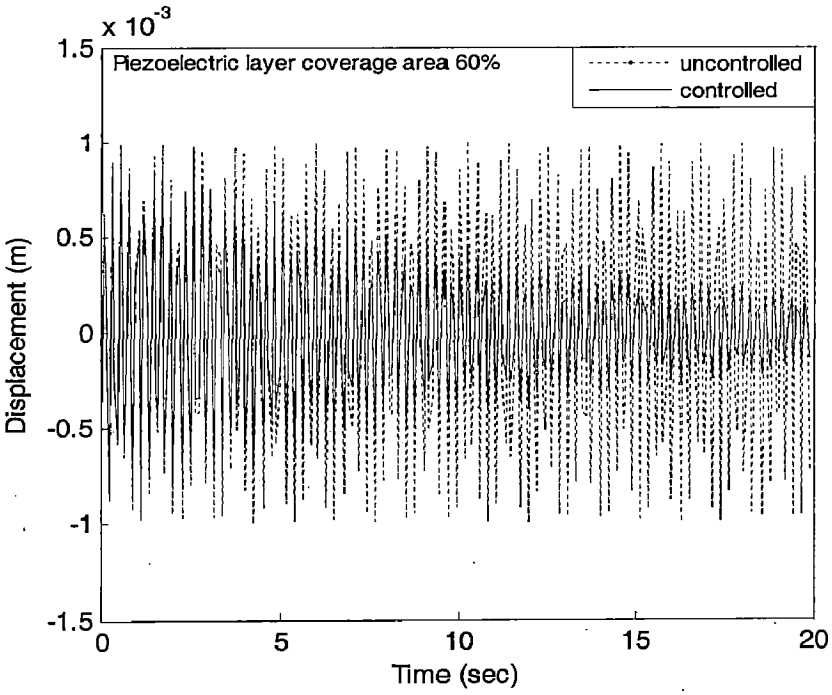

Figure 6.15 (b)

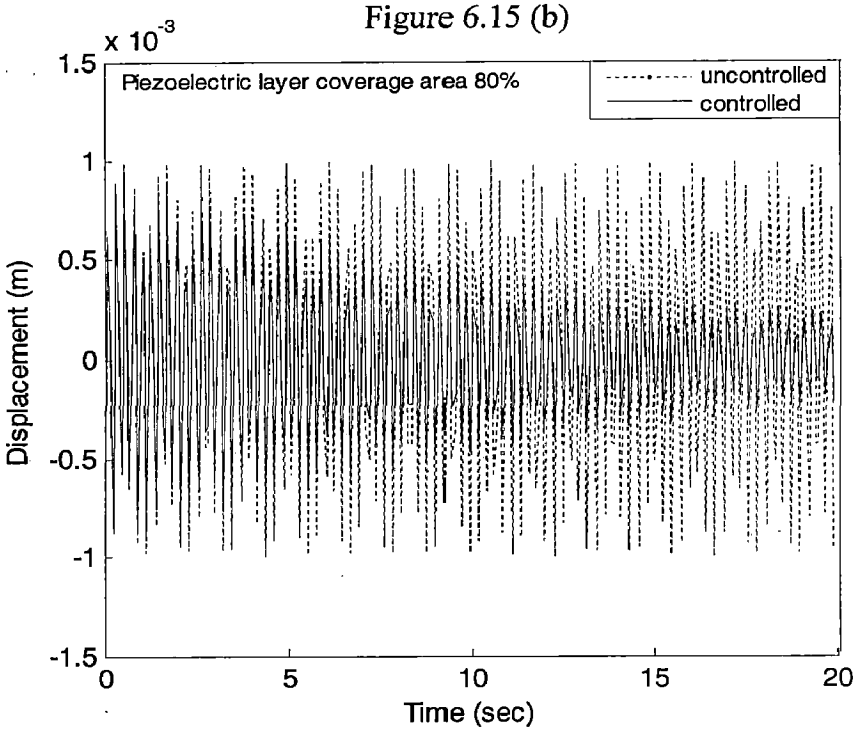

Figure 6.15 (c)

Fig.6.15 (a), (b) and (c) shows the tip responses in hoop direction at 40%, 60% and 80% of piezoelectric layer coverage area from fixed end respectively for a specific gain G=150. It is observed that at 40% piezolayer coverage area the vibration decay is as good as for at 60% and 80% and hence there is no necessary to increase percentage of piezolayers coverage area more than 40% from fixed end for vibration control. It is also

observed that better vibration control is obtained for small percentage of piezolayers coverage area from fixed end as compared to piezolayers coverage area from free end.

6.3 Control using Neural Network

First the model in neural network is developed for identification of the structure and for control of the structure using BP algorithm with the literature.

6.3.1 Validation of Neural Network model

Both model neural network model and total neural network model is validated with the literature [31].

Problem

The dynamics of a nonlinear plant or structure is given by the following second-order difference equation

$$y_p(k+1) = \frac{y_p(k)y_p(k-1)[y_p(k)+2.5]}{1+y_p^{\,2}(k)+y_p^{\,2}(k-1)} + u(k) \qquad (6.1)$$

where

where $u(k)$ is the input to the plant.

Let us assume that we need to design a neural network controller (Neuro-controller) so that the overall behaviour of the controlled system can be described by the reference model equation, given as:

$$y_m(k+1) = 0.6y_m(k) + 0.2y_m(k-1) + r(k) \qquad (6.2)$$

where

$r(k)$ is the reference input to the controller.

Identification (Model Neural Network)

In the identification stage, the unknown plant is identified off line using random input $u(k)$ by a neural network which is known as model neural network (MNET). The input parameters for model neural network are given in Table 6.8. During training, the difference between the output of model neural network and the desired output is minimized to adjust the connective weights in the multi-layered neural network. Training block diagram of the model neural network is shown in fig. 6.16.

Table 6.8

Network Initialization	Model Neural Network
Inputs	2
Outputs	1
Layers	3
Neurons per layer	[20, 10, 1]
Steps of training	500
Error goal	4×10^{-8}

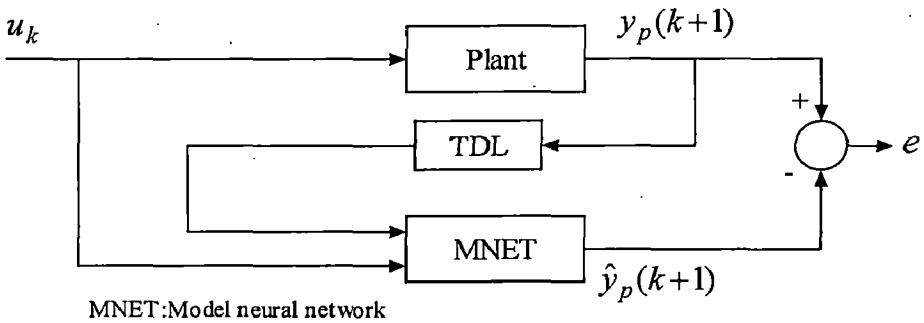

Figure 6.16 Training block diagram of MNET

1. Generation of input/output pattern

Input patterns are taken within the range [-2, 2] and corresponding output patterns generated using eq. 6.1. Fig 6.17 (a) and fig 6.17 (b) shows input/output pattern for training the model neural network.

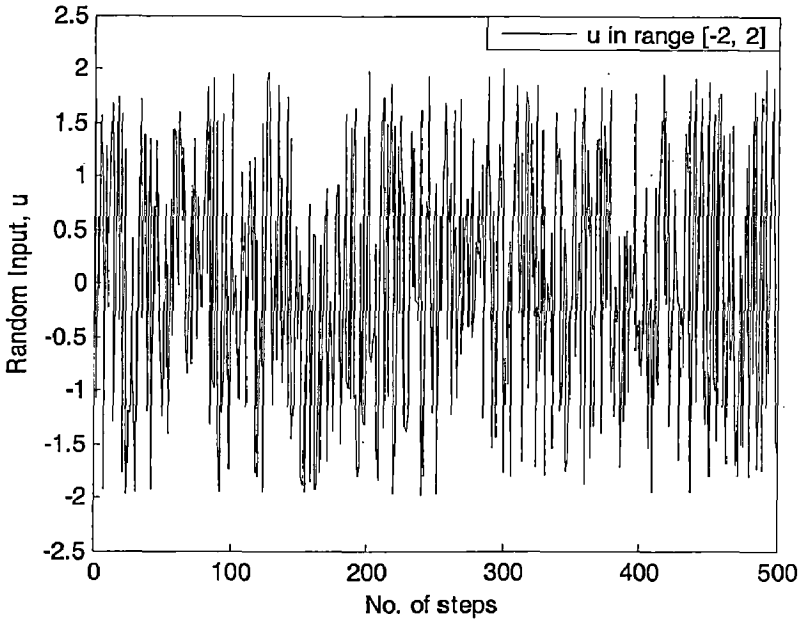

Figure 6.17 (a)

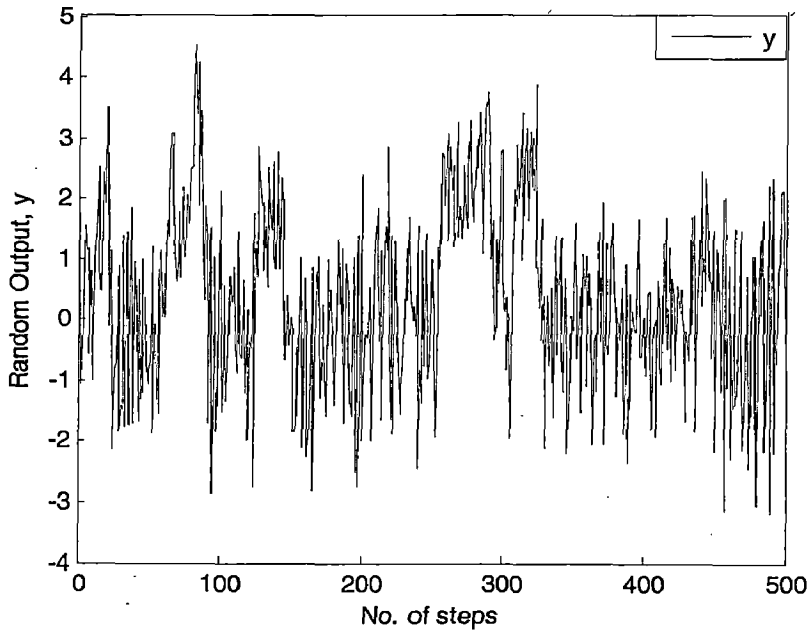

Figure 6.17 (b)

2. Training of Model Neural Network

The error between the output of the model neural network and desired output is minimized during the training. Fig. 6.18 shows the plot of errors versus number of epochs during the training. From the fig. 6.18 it is clear that goal is achieved at 727^{th} epoch

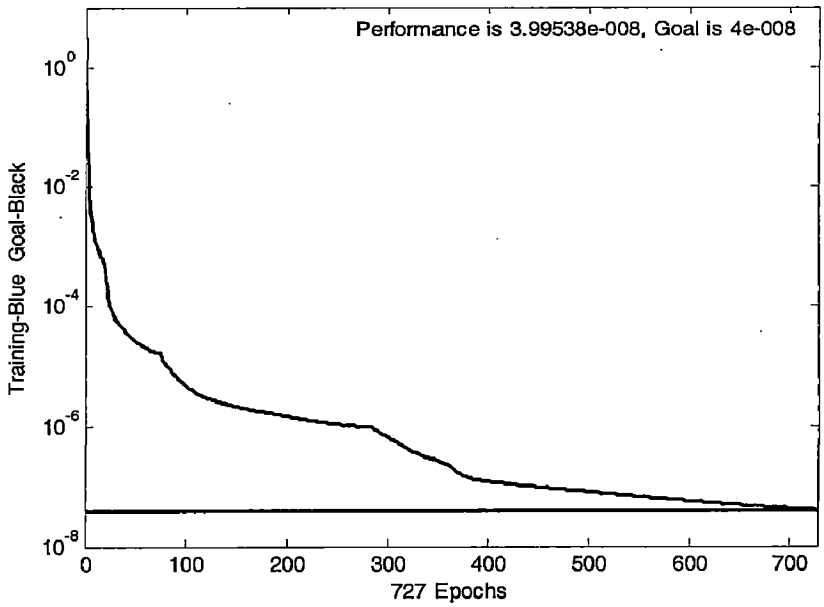

Figure 6.18

3. Testing of Model Neural Network

For the testing of the Model Neural Network, the results are checked for unknown input. Let unknown input is defined as

$$u(k) = \sin(2\pi k / 25)$$

The unknown input pattern $u(k)$ is calculated for 100 number of steps. The output for this unknown input is calculated by two methods.

1. *Analytically.* By using eq. (6.1)
2. *Using Model Neural Network.*

Fig. 6.19 shows the output of model neural network coincides with plant output very well.

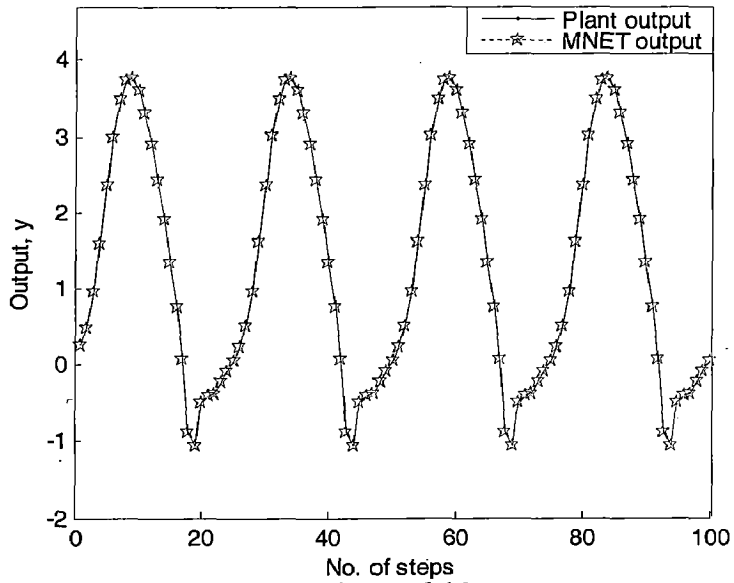

Figure 6.19

Neural Network Controller

Neural network controller (CNET) generates a controlled signal, which is fed to the plant. There are three controller inputs: reference inputs, delayed controller outputs and delayed plant/ structure outputs.

The input parameters for controller neural network are shown in Table 6.9.

Table 6.9

Network Initialization	Controller Neural Network
Inputs	3
Outputs	1
Layers	3
Neurons per layer	[30, 10, 1]

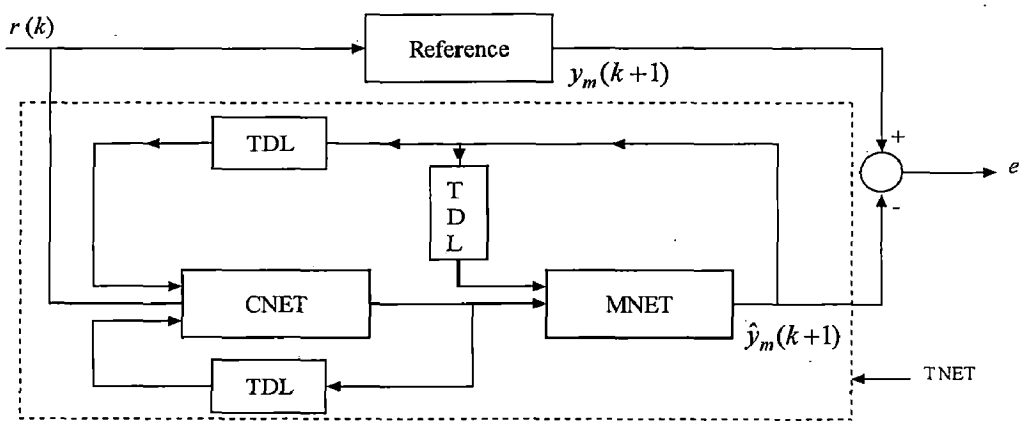

Figure 6.20

Total Neural Network (TNET)

The training of neural network controller can be done on the structure with the aid of model neural network. The combination of neural network controller and model neural network is known as Total neural network (TNET). The training block diagram of the neural network controller with the aid of the model neural network is shown in fig.6.20. The input parameters of Total neural network are shown in Table 6.10.

Table 6.10

Network Initialization	Total Neural Network
Inputs	3
Outputs	1
Layers	6
Neurons per layer	[20, 10, 1, 30, 10, 1]
Steps of training	500
Error goal	2×10^{-5}

1. Generation of input/output pattern

Input patterns for training the controller neural network are also taken within the range [-2, 2] and corresponding output patterns generated using eq. 6.2. Generated input/output patterns are shown in fig 6.21 (a) and fig 6.21 (b) respectively.

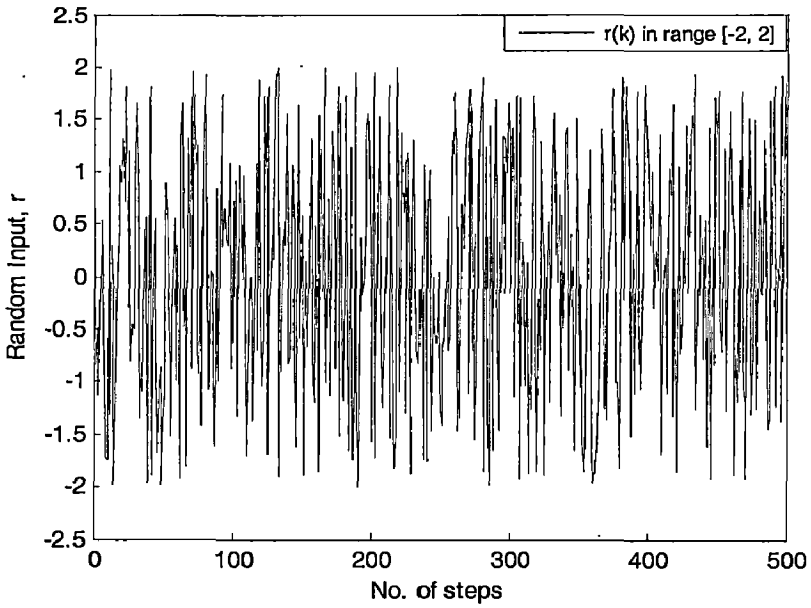

Figure 6.21 (a)

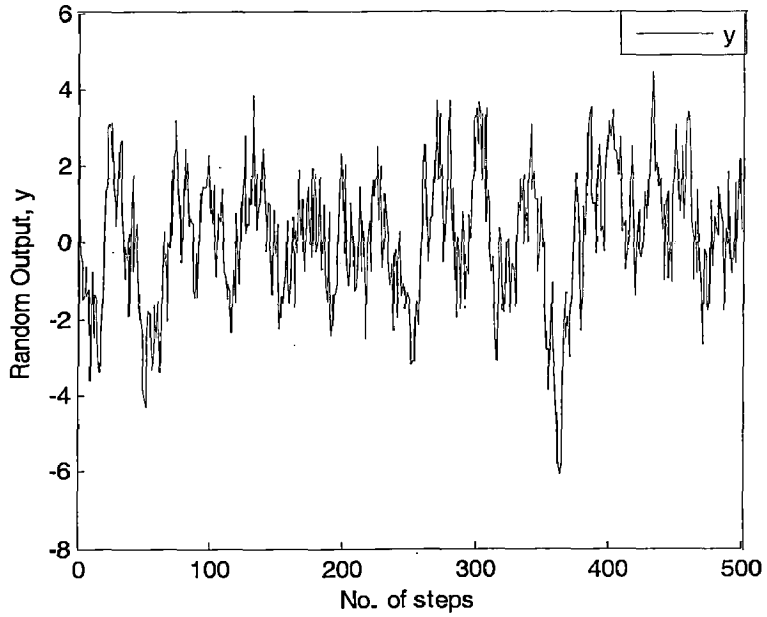

Figure 6.21 (b)

2. Training of Total Neural Network Model

The error between the output of the total neural network and desired output (reference model output) is minimized during the training of total neural network. Fig. 6.22 shows the plot of errors versus number of epochs during the training. From the fig. 6.22 it is clear that goal is achieved at 1600^{th} epoch

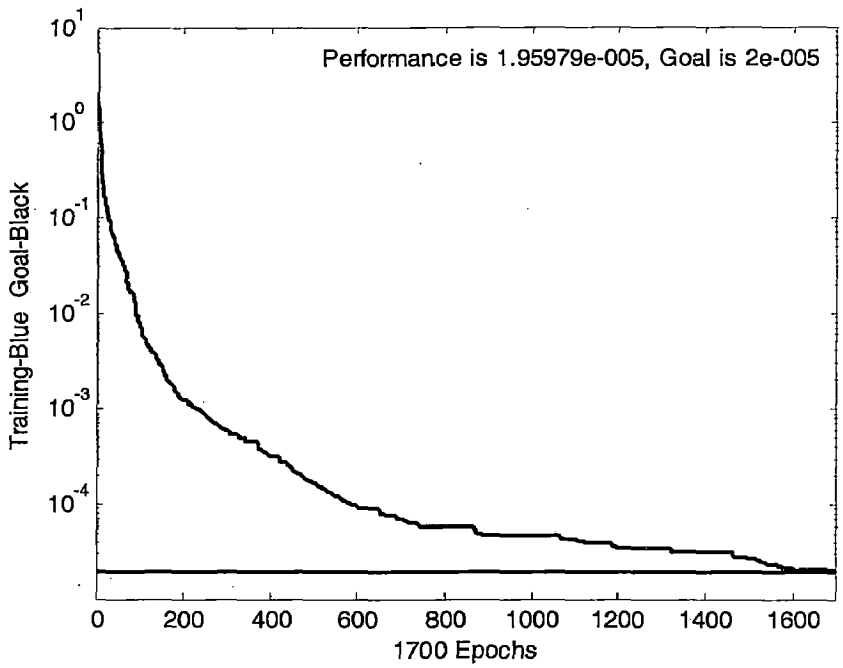

Figure 6.22

3. Testing of Total Neural Network Model

For the testing of the Total Neural Network Model, let unknown reference input is defined as

$$r(k) = \sin(2\pi k / 25)$$

The unknown input pattern $r(k)$ is calculated for 100 number of steps. The output for this unknown input is calculated by two methods.

3. *Analytically*. By using eq. (6.2)
4. *Using Total Neural Network Model*

The output of the total neural network along with the analytical output is shown in fig.6.23 and it shows that output of total neural network coincides with reference model very well.

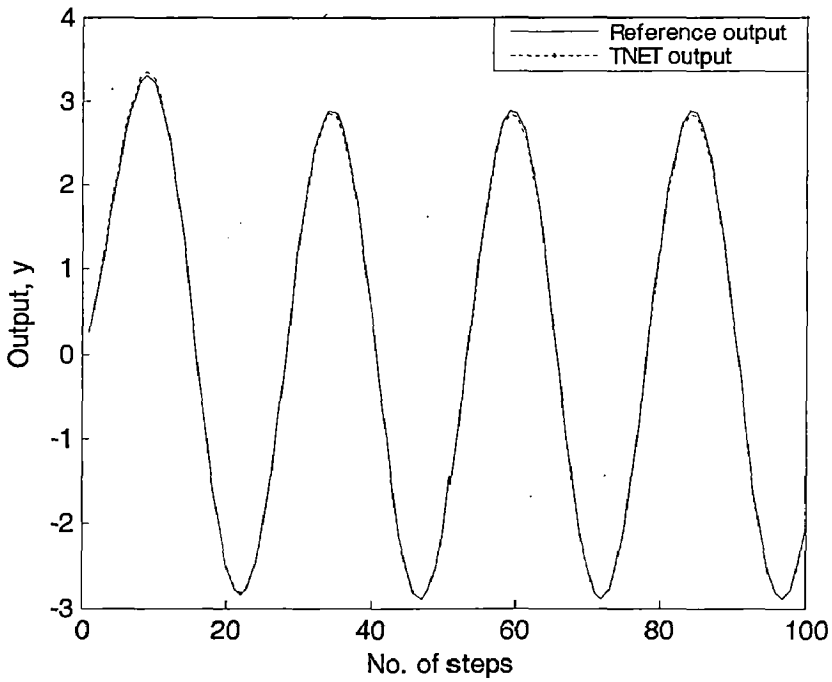

Figure 6.23

Two case studies are considered. In first case study, effect of less number of time steps on training is studied and in second case study, effect of number of neurons on training is studied.

6.3.2 Case 1. Effect of using less number of time steps for training of identification and control model

Number of time steps used for training of identification and control model = 50

Number of time steps used for testing unknown input =100

Identification

1. Training of Model Neural Network

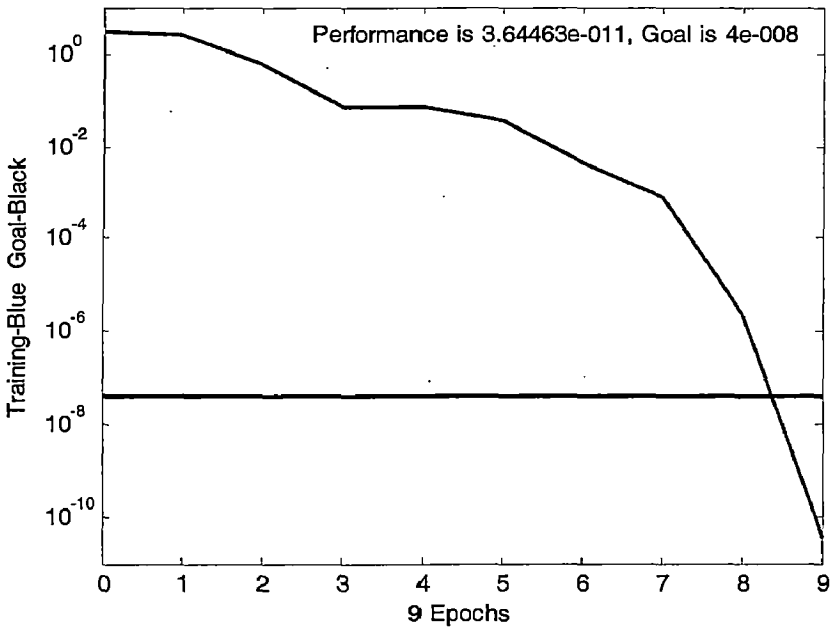

Figure 6.24

2. Testing for unknown input

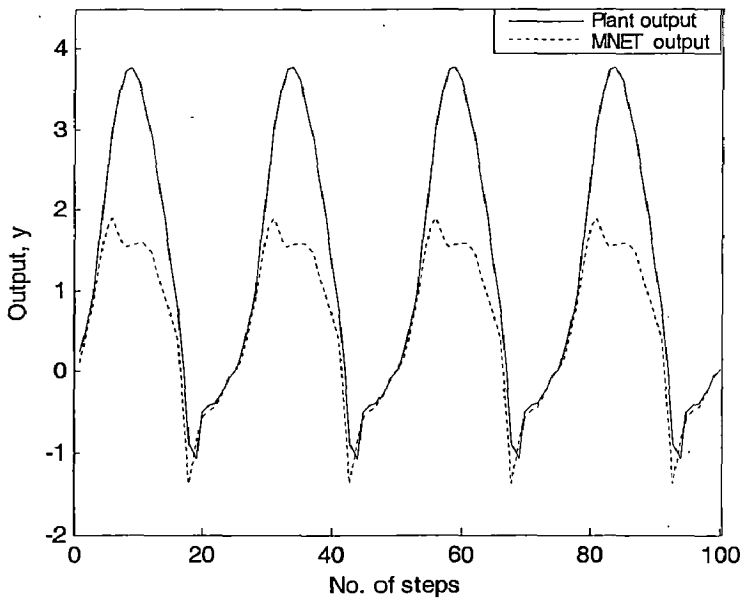

Figure 6.25

From fig. 6.25, it is observed that the output of model neural network does not coincide with plant output. This study suggests that, number of steps should be taken more as much as possible for correct identification. On the other hand for large number of time steps, training time will be large.

Control

1. Training of Total Neural Network

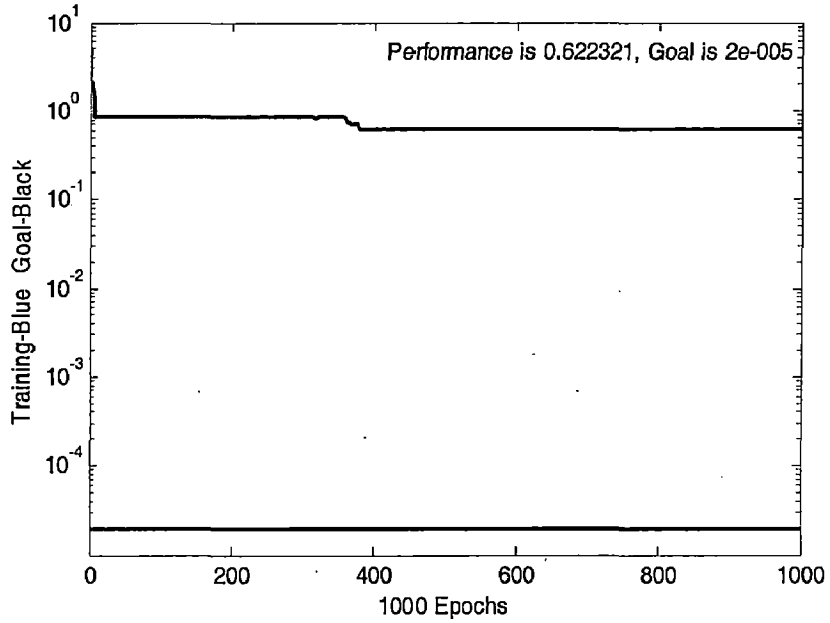

Figure 6.26

2. Testing of Total Neural Network

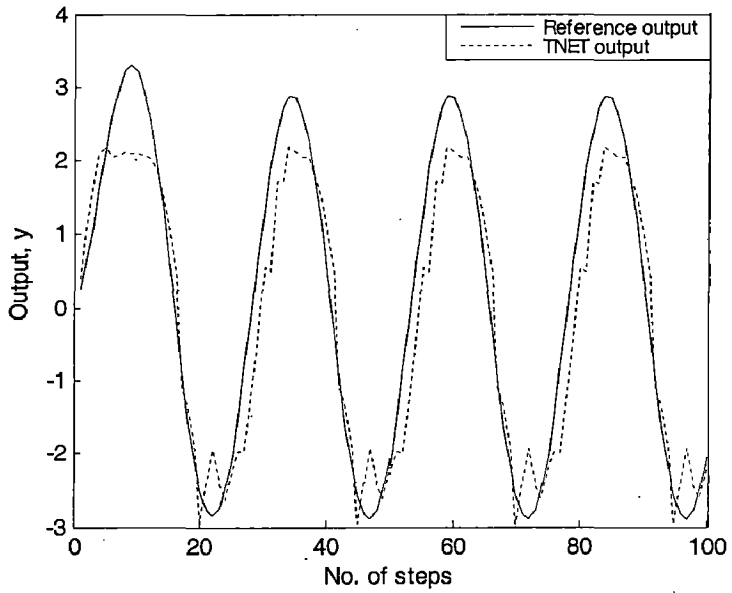

Figure 6.27

It is observed that from the fig. 6.26, that training is not complete for less number of time steps. Fig. 6.27 shows that output of TNET does not coincide with the reference output. This study suggests that for correct controlling, number of steps should be taken more as much as possible.

6.3.3 Case 2. Effect of increasing number of neurons in Model Neural Network and Total Neural Network

Number of neurons in 3 layer Model Neural Network = [24, 10, 1]

Number of neurons in 3 layer Neural Network Controller = [34, 20, 1]

Identification

1. Training of model neural network

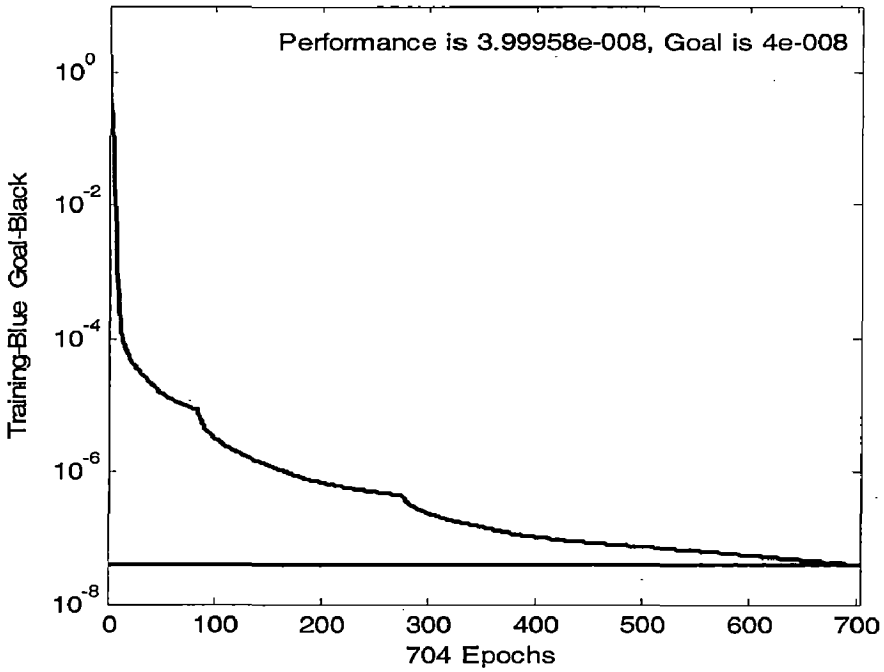

Figure 6.28

2. Testing for unknown input

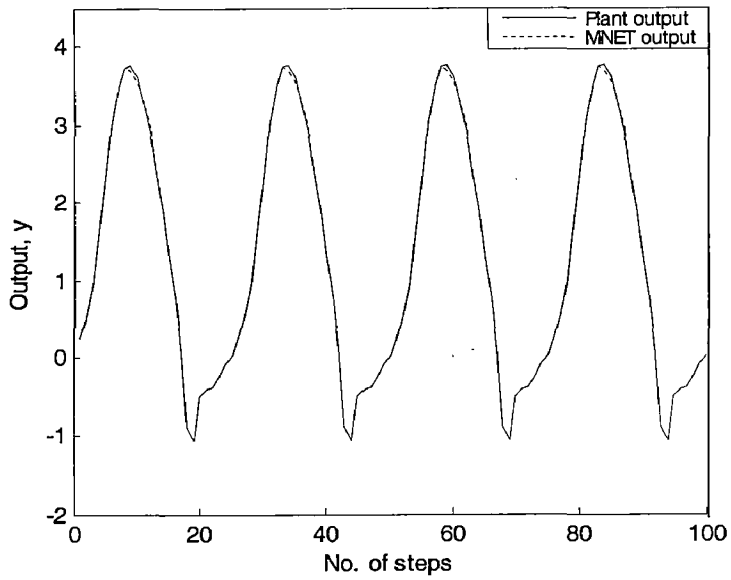

Figure 6.29

It is observed from fig 6.28 that as the number of neurons are increased in layer [20, 10, 1] to [24, 10, 1], goal achieves at less number of epoch (690^{th} epoch). Fig. 6.29 shows that output of MNET deeply coincides with plant output.

Control

1. Training of Total Neural Network

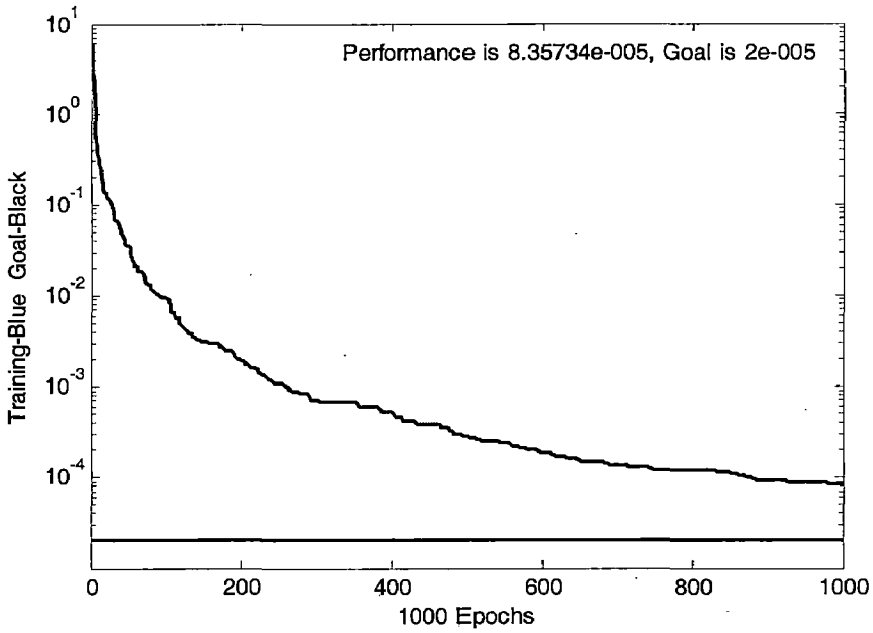

Figure 6.30

2. Testing of Total Neural Network

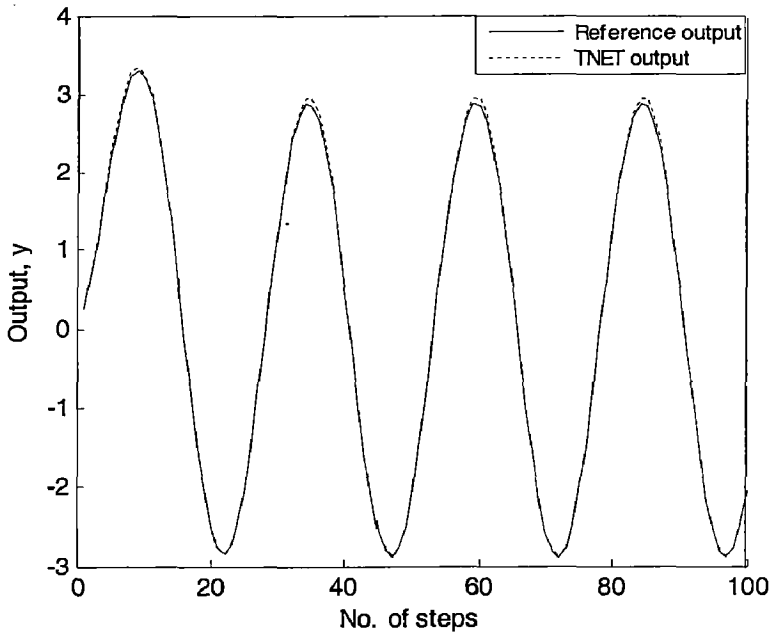

Figure 6.31

It is observed from fig 6.30 that as the number of neurons are increased in layer [30, 20, 1] to [34, 20, 1], goal achieves at less number of epoch. Fig. 6.31 shows that output of TNET deeply coincides with reference output.

CHAPTER 7

CONCLUSION AND SCOPE FOR FUTURE WORK

7.1 Conclusion

In this work a finite element model of piezolaminated composite curved beam based on Timoshenko beam model and linear piezoelectric theory is presented. Finite element has three mechanical degree of freedom (u_0, w_0, θ_y) per node and one electrical degree of freedom per piezoelectric layer. Finite element has n-host structure layer and two piezoelectric layers.

In deriving the finite element model of piezolaminated curved beam first displacement equation is given followed by strain displacement relationship, constitutive equation of piezoelectric, force and bending moment relation, strain energy equation, electrical energy equation, work done by external forces and electrical charges, kinetic energy equation. Governing equations are derived using Hamilton's principle.

Finite element model is validated for static and dynamic analysis for with and without piezolayers with the available literature. A neural network controller is developed.

Based on numerical study following conclusion are drawn.

- As the radius of curvature increases tip deflection increases for both symmetric and antisymmetric layered curved beam. For the same radius of curvature tip deflection for symmetric case is more than antisymmetric case. It is because of variation of stiffness with layer orientation angle.
- Piezoelectric actuators can be used as the shape control of the curved beam. It is observed that neutral plane of curved beam of curvature angle 90° regains approximate its undeformed position at 240V, while neutral plane of curved beam of curvature angle 180° regains approximate its undeformed position at 260V.
- As the coverage area of actuator increases from the fixed end tip deflection increases, deflection increases fastly as the coverage area increases up to 40% beyond this, deflection increases slowly. It is because of more stress develops at the fixed end.

- As the coverage area of actuator increases from the free end tip deflection increases uniformly. It is because of more stress develops at the fixed end.
- Natural frequency of piezolaminated layered curved beam decreases as the radius of curvature increases for both symmetric and antisymmetric layers. However, natural frequency is more in case of antisymmetric composite curved beam compared to symmetric curved beam. It is because of decreasing the stiffness/mass ratio.
- It is observed that decay of vibration is fast at high constant gain. It is because of increasing effective damping. It is also observed that constant gain negative velocity feedback controllers is asmoptically stable. It is because of amplitude of vibration decreases with time.
- It is observed that for 40% piezolayer coverage area, vibration decay rate is same as for at 60% and 80% coverage area. It suggests that it will be uneconomical to increase percentage of piezolayers coverage area more than 40% from fixed end for vibration control. The reason of this is high stress develop at fixed end.
- It is also observed that better vibration control is obtained for small percentage of piezolayers coverage area from fixed end in compare to piezolayers coverage area from free end. It is because of high stress develop at fixed end.
- Constant gain negative velocity feedback controller is suitable for linear control application, while neuro-controller may be used for both linear and nonlinear control applications. It is because of neuro-controller depends on training.
- Number of time steps used for training the neural network controller effects the control operation. It is suggested that number of time steps should be large as much as possible. So that sufficient number of input/output patterns should be there to train model neural network and controller neural network.
- Number of neuron in model neural network (MNET) and neural network controller (CNET) also effect the identification and control application.

7.2 Scope for future work

- Developed finite element model of layered curved beam can be extended to validate experimentally.
- Developed finite element model of layered curved beam can be extended to account the viscoelastic effect between the adjacent layers.
- Developed finite element model of layered curved beam can be extended to account temperature effect in order to include the pyroelectric effect and thermal-strain effect.
- Classical negative velocity feedback controller can be replaced with the developed neuro-controller to control the vibration.
- Optimum configuration and location patches should be decided to control the vibration.

REFERENCES

[1] A.V. Shrinivasan and D.Michael McFarland, 2001, "Smart Structures Analysis and Design", The Press Syndicate of The University of Cambridge.

[2] Xiang Zheng, Argyrios Zolotas, Roger Goodall, 2005, "Smart Materials for Active Control of Flexible Structures in Railway Vehicles", www.lboro.ac.uk/departments/el/research/conferences/esc2005/Xiang_Zheng.pdf

[3] Juhi Khanna, 2004, "Modeling and Control of Smart Cantilever Beam", MTech thesis, IIT Bombay.

[4] A. Preumont, May 2001, "Active Vibration Control", Lecture notes on Structural Control and Health Monitoring (SMART'01), pp. 13-53.

[5] Anabd K.Asundi, "Smart Structures Research at NTU", www.media.mit.edu/resenv/classes/MAS965/readings/SmartStructuresOverview.pdf

[6] J.N.Reddy, 1998, "Theory and Analysis of Elastic Plates", Taylor & Francis.

[7] J.N. Reddy, 1984, "Energy and Variational Methods in Applied Mechanics", John Wiley.

[8] Sudhakar A. Kulkarni and Kamal M. Bajoria, 2003, "Finite Element Modeling of Smart Plates/Shells Using Higher Order Shear Deformation Theory", *Composite Structures*, Vol.62, pp.41-50.

[9] V Balamurugan and S Narayanan, 2003, "Finite Element Modeling of Piezolaminated Smart Structures for Active Vibration Control with Distributed Sensors and Actuators", *Journal of Sound and Vibration*, Vol.262, pp.529-562.

[10] Singiresu S.Rao, 2005, "Mechanical Vibrations", Pearson Education (Singapore) Pvt.Ltd

[11] Haykin, Simon, 1994, "Neural Networks: A Comprehensive Foundation", Cambridge University Press.

[12] S.Rajasekaran, G.A. Vijayalakshmi Pai, 2004, "Neural Networks, Fuzzy Logic, and Genetic Algorithms Synthesis and Applications", prentice-hall of India.

[13] Martin T.Hagan, Howard B. Demuth, "Neural Networks for Control", www.hagan.okstate.edu/HaganDemuthACC99.pdf

[14] Gwo-Shing Lee, 1996, "System Identification and Control of Smart Structures Using Neural Networks", *Acta Astronautica*, Vol.38, pp.269-276.

[15] I.J.Nagrath, M.Gopal, 1999, "Control Systems Engineering", New Age International (p) Llimited, Publishers.

[16] I. A. Bashir, M. Hajeer, 2000, "Artificial Neural Networks: Fundamentals, Computing, Design and Appliacation, *Journal of Microbilogical Methods*, Vol. 43, pp.3-31.

[17] Ratneshwar jha and Chengli He, 2004, "A Comparative Study of Neural and Conventional Adaptive Predictive Controllers for Vibration Suppression", *Smart Materials and Structures*, Vol. 13, pp.811-818.

[18] M. Ananada Rao, 2003, "Neural Networks Algorithms and Applications", Narosa publishing house.

[19] Hui-Rui Shih, 2000, "Distributed Vibration Sensing and Control of a Piezoelectric Laminated Curved Beam". *Smart Materials and Structures*, Vol. 9, pp.761-766.

[20] D.H.Ryu, and Wang, K.W., 2002,"Characterization of surface-bonded piezoelectric actuators on curved beams", *Smart Materials and Structures*, Vol.11, pp.377-388.

[21] D.Chakravorty and J.N.Bandyopadhay, 1995, "Finite Element Free Vibration Analysis of Point Supported Laminated Composite Cylindrical Shells", *Journal of Sound and Vibration,* Vol.181, pp.43-52.

[22] V.Balamurugan, S.Narayanan, 2001, "Shell Finite Element for Smart Piezoelectric Composite Plate/Shell Structures and its Application to the Study of Active Vibration Control", *Finite Elements in Analysis and Design*, Vol.37, pp.713-738.

[23] P. Seshu, V. K. Gupta, 2002, "Finite Element and Experimental Studies on Piezoelectric Actuated Curved Beams", *AIAA Journal, Structures, Structural Dynamics, and Material Conference.*

[24] Snyder and Tanaka, 1993, "A Neural network feedforward controlled smart structures", *Journal of intelligent material systems and structures*, Vol.4, pp.373-378.

[25] Chen ef al, 1994, "Active Vibration Control Using the Modified Independent Modal Space Control (M.I.M.S.C.) Algorithm and Neural Networks as State Estimators", *Journal of intelligent material systems and structures*, Vol.5, pp.550-558.

[26] Vital Rao and Damle et al, 1994, "Identification and Control of Smart Structures Using Neural Networks: A Survey", *IEEE, Proceedings of the 33rd Conference on Decision and Control,* pp.91-96.

[27] Yi-Kwei Wen, Jamshid Ghaboussi, Paolo Venini and Khashayar Nikzad,1995, "Control of Structures Using Neural Networks", *Smart Materials, Structures*, Vol.4, pp.149-157.

[28] J James Douglas Schieffer and Kelvin Erickson, 1995, "Vibration Control in Cantilever Beam Using Neurocontroller", *Journal of intelligent engineering systems*, Vol.5, pp.593-598.

[29] K.Chandrashekhara, M.T.Valoor and S.Agarwal, 1999, "Self Adaptive Vibration Control of Smart Composite Beams Using Hybrid Neural Architecture", *International conference on Smart Materials, Structure*, pp.449-454.

[30] Ratneshwar jha and Chengli He, 2004, "Adaptive Neuro-controllers for Vibration Suppression of Nonlinear and Time Varying Structures", *Journal of intelligent material systems and structures*, Vol.15, pp.771-781.

[31] Kumpathi S.Narendra, 1990, "Identification and Control of Dynamical Systems Using Neural Networks", *IEEE transactions on Neural Networks*, Vol. 1, No. 1, pp.4-27.

[32] M.H.H. Shen, 1995, "A New Modeling Technique for Piezoelectrically Actuated Beams, *Computers and Structures*, Vol. 57, pp. 361-366.

[33] Stephan J. Chapman, 2005, "MATLAB Programming for Engineers", Thomson Asia Pvt. Ltd., Singapore.

Appendix:A Flow Chart of the MAIN programme

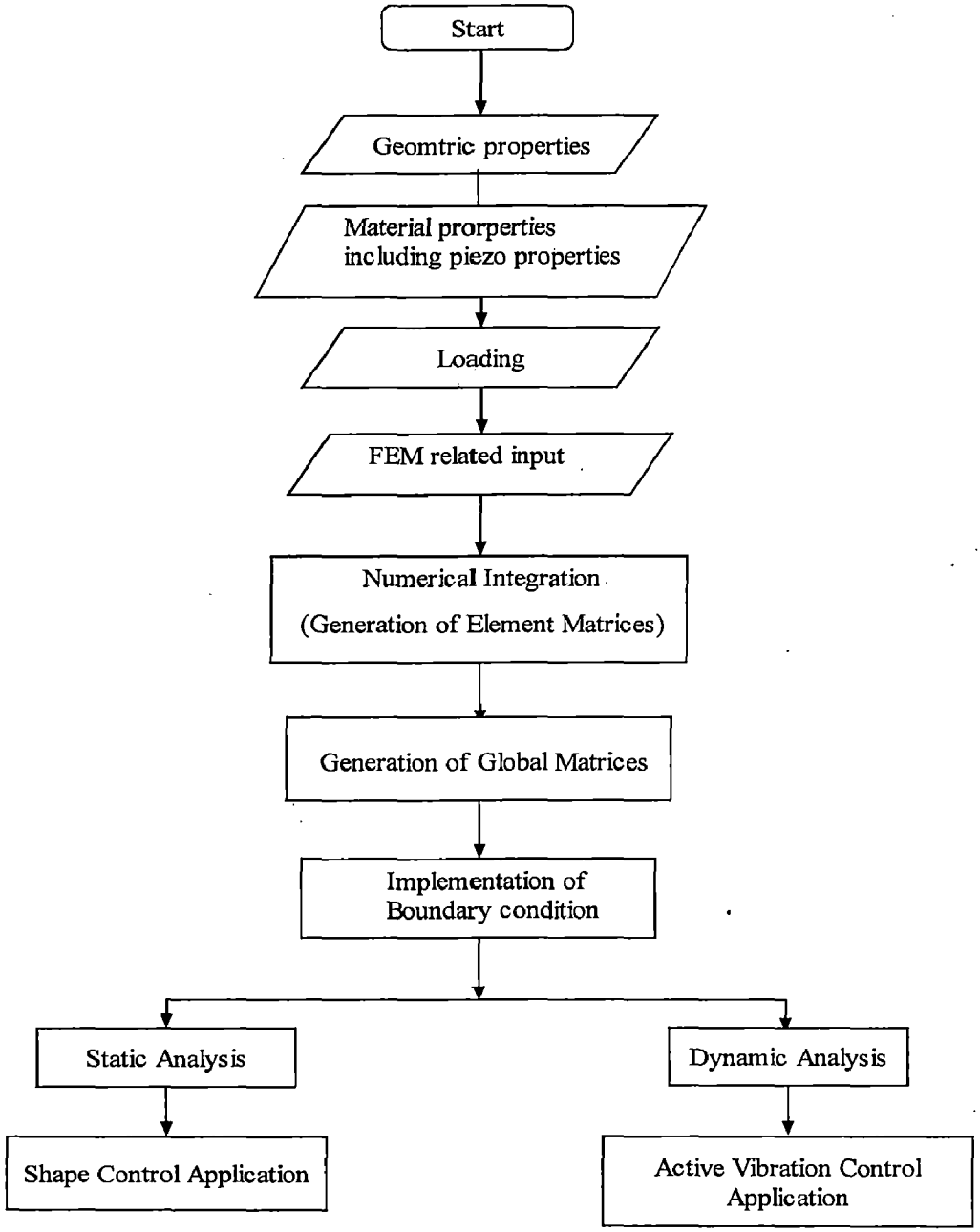

Appendix:B Flow Chart of the Shape Control Application

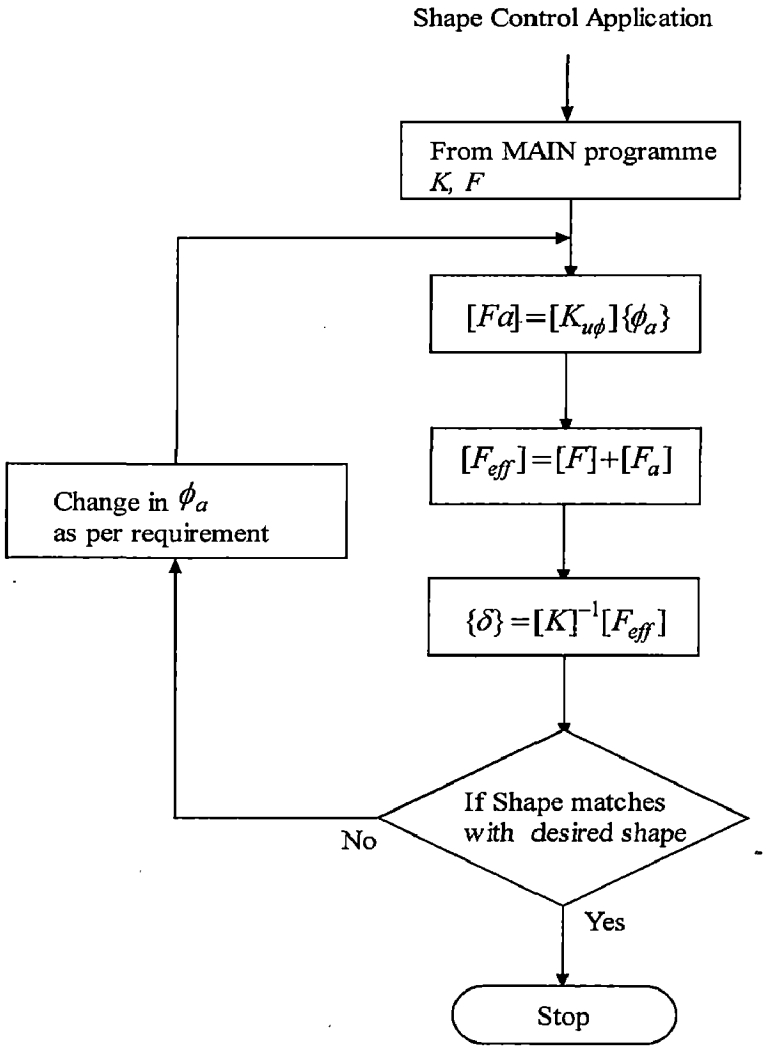

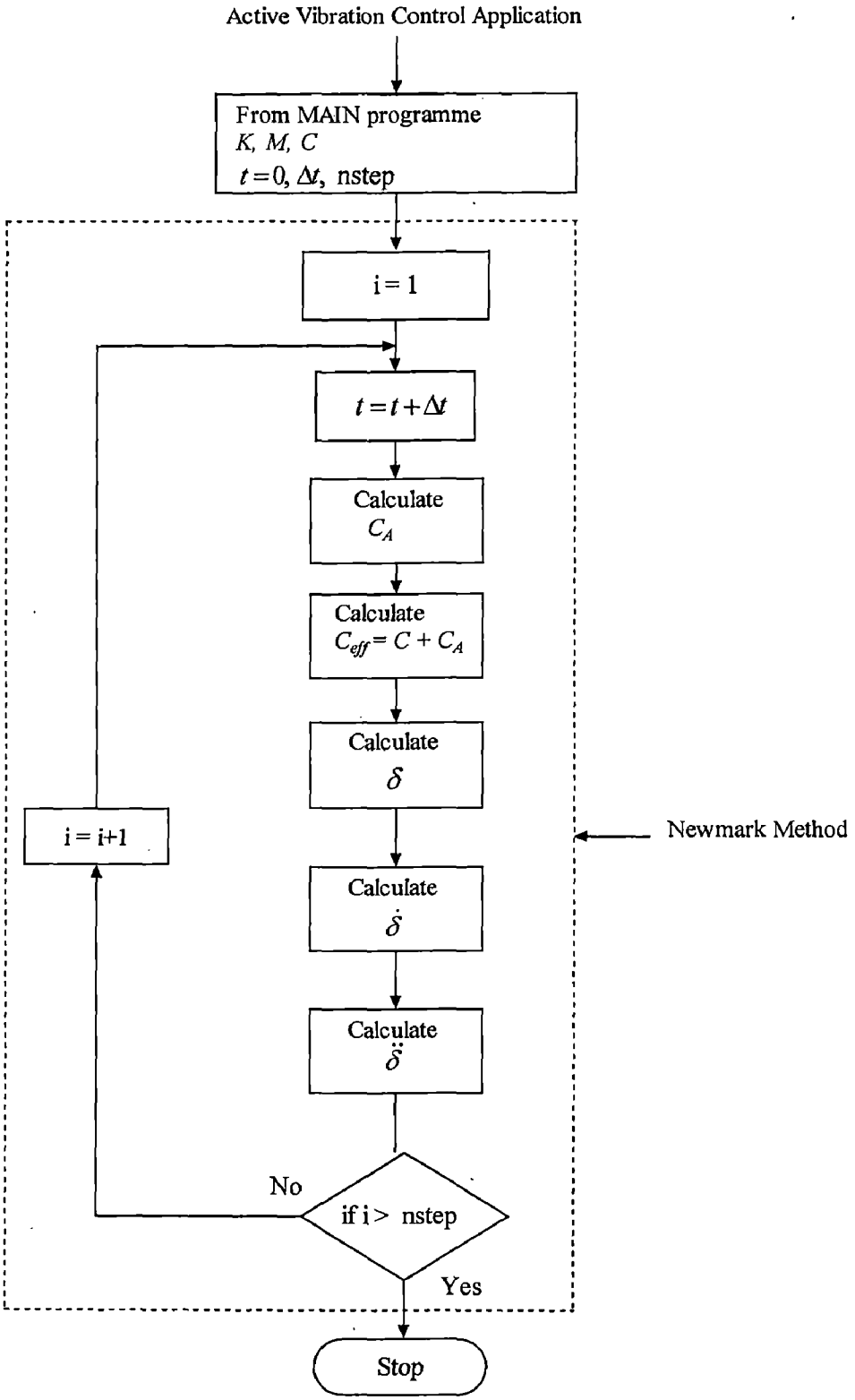
Active Vibration Control Application
From MAIN programme
K, M, C
t = 0, Δt, nstep
i = 1
t = t + Δt
Calculate
C_A
Calculate
C_eff = C + C_A
Calculate
δ
Calculate
δ̇
Calculate
δ̈
if i > nstep
No
Yes
i = i+1
Stop
Newmark Method